DOKUZ EYLÜL UNIVERSITY

GRADUATE SCHOOL OF NATURAL AND APPLIED SCIENCES

HYSTERETIC RESPONSE CHARACTERISTICS OF THE ISING-TYPE NANOMAGNETIC MATERIALS

by

Bahadır Ozan AKTAŞ

June, 2015

İZMİR

HYSTERETIC RESPONSE CHARACTERISTICS OF THE ISING-TYPE NANOMAGNETIC MATERIALS

A Thesis Submitted to the
Graduate School of Natural And Applied Sciences of Dokuz Eylül University
In Partial Fulfillment of the Requirements for the Degree of Doctor of Philosophy in Physics

by

Bahadır Ozan AKTAŞ

June, 2015
İZMİR

Ph.D. THESIS EXAMINATION RESULT FORM

We have read the thesis entitled "**HYSTERETIC RESPONSE CHARACTERISTICS OF THE ISING-TYPE NANOMAGNETIC MATERIALS**" completed by **BAHADIR OZAN AKTAŞ** under supervision of **PROF. DR. HAMZA POLAT** and we certify that in our opinion it is fully adequate, in scope and in quality, as a thesis for the degree of Doctor of Philosophy.

.....

Prof. Dr. Hamza POLAT

Supervisor

.....

Prof. Dr. Kadir YURDAKOÇ

Thesis Committee Member

.....

Prof. Dr. Cesur EKİZ

Thesis Committee Member

.....

Prof. Dr. Nejat Bulut

Examining Committee Member

.....

Prof. Dr. Uğur Tırnaklı

Examining Committee Member

Prof. Dr. Ayşe OKUR
Director
Graduate School of Natural and Applied Sciences

ACKNOWLEDGEMENTS

I would like to thank to my supervisor Prof. Dr. Hamza POLAT. I am also indebted to Assoc. Prof. Dr. Ümit AKINCI for much support, undeniable scientific contributions, endless fruitful discussions somehow we fall into a tautology and mostly finalize with disagreement but also provides me different perspective. I would like to express my special thanks to Celal Cem SARIOĞLU who helped me to get a LaTeX template of manuscript.

I believe that for every PhD candidate near the end of graduation, it is an absolute necessity to express their gratitude to whom push themself beyond what is expected of them in a way or another with no names, face to face.

Finally, inexpressible gratitude is for my dear family, I wish to thank my parents Fatma & Mehmet and my brothers together with their wifes Nurşen & Ali Kubilay and Ayşe & Oğuzhan for their eternal support and encouragement throughout my life. For me, nothing would have been possible without their unconditional love and patience.

The author (BOA) would like to thank the Turkish Education Foundation (TEV) for financial support. The numerical calculations reported in this thesis report were performed at TÜBİTAK ULAKBİM, High Performance and Grid Computing Center (TR-Grid e-Infrastructure).

Bahadır Ozan AKTAŞ

HYSTERETIC RESPONSE CHARACTERISTICS OF THE ISING-TYPE NANOMAGNETIC MATERIALS

ABSTRACT

The conceptual frame of the surface enhancement phenomenon on finite magnetic materials, especially on thin-films and semi-finite systems, has not lost its currency yet and recently there has been growing interest for this mature subject of solid state physics because a variety of apparently very different phenomena can be described by both experimentalists and theorists.

This thesis deals with the hysteretic features of Ising-type thin films under external oscillatory magnetic field. Throughout the analysis, the most appropriate parameter values are chosen since they would allow us to observe the reversed magnetic hysteresis after a certain value of external field frequency. This eccentric phenomenon has prompted us to associate it to the domain nucleation and growth mechanism. The exotic shapes of the response in two different regimes of modified surface exchange are particulary emphasized.

The results are essentially based on two related papers of us including aforementioned systems: By means of effective field theory (EFT), dynamical phase diagrams of Ising-typed pure crystalline thin-films with different thicknesses have been presented. An attempt is made to explain the relations between the competing time scales (intrinsic microscopic relaxation time of the system and the time period of the external oscillatory field) and frequency dispersion of the critical temperature coordinate of the special point. In order to elucidate the nature of hysteresis characteristics in a magnetic Ising-type thin film with a certain thickness, such as types of frequency dispersion curves, corresponding coercive field and remanent magnetization values, etc. have also been propounded in other complementary work.

Keywords: Dynamic critical behavior, Thin-film, Surface enhancement phenomenon, Effective-field theory.

ISING-TİPİ NANOMANYETİK MALZEMELERİN HİSTERETİK YANIT KARAKTERİSTİKLERİ

ÖZ

Sonlu manyetik malzemeler; özellikle yarı-sonsuz ve ince-film sistemlerinde; yüzeyce geliştirilmiş fenomene ilgi geçerliliği kaybetmemiş ve halen artan bir eğilimle deneyciler ve teorisyenler tarafından katıhal fiziğinin bu olgunlaşmış öğesi incelenmektedir.

Bu tez çalışması salınımlı bir dış manyetik alan altındaki Ising-tipi ince filmlerin histeretik yanıt özellikleri üzerinedir. Analiz boyunca en uygun parametre değerleri özenli bir biçimde seçilmiştir, ki bu bize dış alanın belirli bir frekans değerinden sonraki değerinde terslenmiş manyetik histeresizin gözlemlenmesine olanak sağlamaktadır. Bulgularımız bizi, bu sıradışı fenomeni domen çekirdeklenmesi ve gelişimi mekanizması ile ilişkilendirmeye sevketmiştir. Modifiye edilmiş yüzey değiş-tokuş parametresinin iki farklı rejiminde söz konusu yanıtın egzotik şekli ayrıca incelenmiştir.

Sonuçlar yukarida sözü geçen sistemleri içeren iki makaleye dayanmaktadır: Farklı kalınlıklardaki Ising-tipi pür kristal ince-filme ait dinamik faz diyagramları etkin-alan teorisi (EAT) ile ortaya koyulmuştur. Özel noktanın kritik sıcaklık koordinatına ait frekans dispersiyonu ile rekabet halindeki zaman ölçekleri (sistemin mikroskopik içsel durulma zamanı ile dış alanın periyodu) arasındaki ilişkinin ortaya koyulmasına yönelik bir girişimde bulunulmuştur. Belirli bir kalınlıktaki Ising-tipi manyetik ince filmde frekans dispersiyonu tipleri, karşı gelen koersif alan ve remanent manyetizasyon değerleri, vb. gibi histeresiz karakteristiklerinin doğasının aydınlatılması için tamamlayıcı bir diğer çalışma da ayrıca ortaya koyulmuştur.

Anahtar kelimeler: Dinamik kritik davranış, İnce-film, Yüzeyce geliştirilmiş fenomen, Etkin-alan teorisi.

CONTENTS

Page

LIST OF FIGURES

Page

CHAPTER ONE
BASIC CONCEPTS AND BEYOND

As an introductory overview of this thesis, we first plan to give a picture of dynamical phase transition, hysteresis characteristics and the magnetic systems under consideration.

1.1 Prologue

Since the time in which Ising model (Ising, 1925) was invented there exists a limited number of studies including the dynamic nature of the system under the influence a time dependent oscillating magnetic field. Even though the physical investigations regarding these systems bring about a lot of mathematical difficulties, the nonequilibrium systems are in the focus of scientists because they have an unusual and interesting dynamic behavior. By using the kinetic Ising model, the first calculation was performed by Tomé and Oliviera (Tomé & de Oliveira, 1990) benefiting from Glauber-type stochastic dynamics (Glauber, 1963). They investigated the time dependence of the magnetization and the temperature dependence of the dynamic order parameter (DOP) which is defined as the time averaged magnetization over a full cycle of the oscillating magnetic field the mean field approximation (MFA). From these calculations, they obtained the dynamic phase transition (DPT) points and they drew the dynamic phase boundary (DPB) which separates the dynamic ordered phases from the dynamic disordered phases. They also located a dynamic tricritical point (DTCP) at which the type of phase transition change across the DPB. Moreover, they analyzed the influence of the frequency of the external field on the DPB.

1.2 Hysteresis

When a cooperative many-body system such as a magnet is subject to an alternating external magnetic field, the ordinary magnetization, in other words, magnetization would oscillates and may not respond to the external field simultaneously. Hence the system exhibits an ubiquitous phenomenon which is called hysteresis. For the kinetic

Ising-type systems, the most familiar hysteresis in the form of lissajous curve and essentially originated from the variation of ordinary (time-dependent magnetization) $m(t)$ of the system versus the external magnetic field $h(t)$. This ubiquitous phenomenon has been subjected of intensive interest due to a broad range of applications.

Applied oscillating magnetic fields, depending on the competition between the two time scales, namely the oscillation period P of the external perturbation and the relaxation time τ of the sample[1], a dynamic symmetry breaking may take place causing a DPT. There are two cases due to the competition between these time scales: $P < \tau$ and $P > \tau$. In the first case, the system cannot relax within a complete cycle of the magnetic field oscillation, hence the instantaneous magnetization $m(t)$ oscillates in time around a nonzero value corresponding to dynamically ordered state (i.e. dynamic ferromagnetic phase). In other case, $m(t)$ can follow the external field with some delay, and the system exhibits a dynamic paramagnetic behavior. The relaxation time t can be controlled by supplied energy with several different ways: The agency of an adjustable parameter such as the field amplitude, strength itself, the type of the exchange interactions, and the temperature. The DPT point can be controlled by tuning mentioned competing factors together with the time period of external field.

1.3 Magnetic Thin-Films and Semi-Infinite Systems

In the past quarter century, some preliminary experimental evidence has been presented for the existence of a surface type of magnetic ordering since the magnetic properties of free surfaces drastically differ from the bulk material, be- cause the free surface breaks the translational symmetry, i.e. surface atoms are embedded in an environment of lower symmetry than that of the inner atoms and consequently the exchange constants between atoms in the surface region may differ from the bulk value.

One of the early experimental studies dating back to the last quarter of the century, was made by Weller et al. (Weller et al., 1985). There exists an empirical inference that the $4f$ spins of surface are not ferromagnetically coupled to the bulk moments. Due

[1] Actually, within the Glauber-type stochastic process, the system evaluates with time scale τ, τ is the switching time for a single spin. See Chapter 2, Section 5.5 for the details.

to this finding, the relevant work involves the discoveries about the understanding of surface-enhanced magnetic order and magnetic surface reconstruction on Gd(0001). Dürr et al. (Dürr et al., 1989) have showed in the same period that the temperature dependence of the long-range order parameter in thin (1-3 ML) films of bcc Fe on Au(100)−including one monolayer−, as measured with spin polarized low energy electron diffraction and spin-polarized secondary electron emission spectroscopy as a complement. Two experimental observations were published in the early of two decades ago. One of them includes an *in situ* magnetic resonance measurements of ultrathin Ni(110) which was prepared in ultrahigh vacuum. Li and Baberschke (Li & Baberschke, 1992) have carried out an investigation to determine the thickness dependence of the critical exponent β and the Curie temperature T_c. They concluded that the existence of a crossover in the magnetic properties of Ni films as a function of thickness and also the critical exponents were determined in their experiment agree very well with the known exponents for a corresponding 2D Ising-typed bulk Ni. In the other one, thickness-dependent Curie temperature of 5-100 monolayers Gd on W(100) and its dependence on the growth conditions are determined by *in situ* ac-susceptibility (χ_{ac}) measurements by Farle et al. (Farle et al., 1993). They found that the Curie temperature of carefully prepared layer-by-layer-grown Gd(0001) films varies from T_c(bulk) = 292.5K to T_c(5ML) = 120K and it was also demonstrated that different growth conditions change the Curie temperature of the film dramatically. After the aforementioned studies, an examination was propounded in the subsequent years by Poulopoulos and Baberschke (Poulopoulos & Baberschke, 1999). They discussed the fundamental magnetic observables, i.e. magnetic moment per atom, Curie temperature, susceptibility and magnetic anisotropy, for idealized prototype thin films like Fe, Co, Ni on metal substrates such as Cu, W, Re. Former experimental measurements suggest the possibility of large surface anisotropies in thin films (Jonker et al., 1986; Pescia et al., 1987a; Pierce, 1987; Pappas et al., 1990). Beside the relevant elements, magnetically ordered surface can exist also for Cr (Rau & Eichner, 1981; Rau et al., 1988). It is avowable that there exists a general phenomenon due to the reduced coordination number, the critical temperature is lower at surface in thin films and decreases with decreasing film thickness (Stampanoni et al., 1987; Przybylski

& Gradmann, 1987; Schneider et al., 1990). As presented by Detzel et al. (Detzel et al., 1996) and Stampanoni et al. (Stampanoni, 1989), for fcc Fe films on Cu(100) substrates, the Curie temperature increases strongly from one to two monolayers, but decreases in thicker layers. For the Fe films grown on Ni/Si substrates, it was observed that a transition between magnetic and nonmagnetic phases occurs at a critical thickness (Edelstein et al., 1990; Krishnan et al., 1991; Colombo et al., 1992; Li et al., 1996). With the recent advances in epitaxial growth techniques (especially in molecular beam epitaxy) it is now possible to grow very thin magnetic films of controllable thickness and this has stimulated renewed interest in both experimental and theoretical film magnetism (Farle & Baberschke, 1987; Pescia et al., 1987b).

Theoretical treatments on the semi-infinite systems and thin films in the literature have continued simultaneously with experiments (Binder & Hohenberg, 1974; Binder, 1974; Aguilera-Granja & Morán-López, 1985; Landau & Binder, 1990; Kaneyoshi, 1991; Wang et al., 1997; Yao et al., 2002; Saber et al., 1999; Laosiritaworn et al., 2004; Cossio et al., 2006; Laosiritaworn, 2009; Park & Pleimling, 2012). Ising models with modified exchange interaction on the surface were considered by Binder and Hohenberg and the critical value of the modified exchange for surface ordering was found from high-temperature-series expansion and compared to MFA value in their work (Binder & Hohenberg, 1974). They reported that there exists a temperature region in which the surface behaves like a two-dimensional Ising-typed bulk near its transition point for the values greater than the critical value of relevant exchange. The average magnetization of the simple cubic Ising films (with different thicknesses) was calculated as a function of temperature using the Monte Carlo (MC) technique by Binder in the same year (Binder, 1974). The semi-infinite Ising model with an arbitrary number of surface magnetic couplings differing from the bulk exchange constant, was solved within the MFA by Aguilera-Granja and Morán-López in the middle of three decades ago (Aguilera-Granja & Morán-López, 1985). They showed that the exact expressions for the critical couplings would lead to a higher surface Curie temperature than the bulk one. Landau and Binder (Landau & Binder, 1990) have performed MC simulations and they have presented the results of phase transitions

and critical behavior at the surface of a simple cubic Ising model. Later on, a review of the surface magnetism was given by Kaneyoshi (Kaneyoshi, 1991). Mainly, the interplay of magnetizations and anisotropy at a surface was discussed in that review. Ferroelectric films were studied to obtain the polarization and the dependence of the Curie temperature on the long-range exponent in two works (Wang et al., 1997; Yao et al., 2002). Parallel study using a distorted lattice was propounded the same dependence of the Curie temperature and polarization by Wang et al. (Wang et al., 1997). Yao et al. (Yao et al., 2002) have presented that the long-range dipole-dipole interaction made the transition temperature higher. In both studies (Wang et al., 1997; Yao et al., 2002), films were described by transverse Ising model (TIM) with long-range interactions. Transverse spin-1/2 Ising film was also examined in detail within the framework of the EFT by Saber et al. (Saber et al., 1999). It was found that if the ratio of the surface interaction to the bulk one is less than a critical value, the critical temperature of the film is smaller than the bulk critical temperature and as the film thickness is increased further, critical temperature increases and approaches asymptotically to the bulk-critical temperature for large values of the thickness. In MC simulations on semi-infinite systems, a linear dimension parameter should be much larger than the other two in order to maintain the quasi two dimensional structure of the films. This detail should also be taken in consideration to preserve the geometry of the film. Within this computational framework, in recent years, Laosiritaworn and co-workers (Laosiritaworn et al., 2004) have used MC simulations and the MFA to observe the magnetic behavior of Ising films with cubic lattice structure as a function of temperature with thickness. They found that the magnetic behavior changes from two-dimensional to the three-dimensional character with increasing film thickness. The same computational technique was used by Cossio et al. (Cossio et al., 2006) to explain the temperature dependence of the magnetization, the magnetic susceptibility and also the fourth-order Binder's cumulant. Ferromagnetic (F) Ising-typed thin film in the presence of a time dependent external oscillatory magnetic field was investigated to model the hysteretic behavior of the system by Laosiritaworn (Laosiritaworn, 2009). In that work, MC simulation was used and thickness dependence of hysteresis properties for varying frequency and amplitude of the external field was investigated.

The study of the surface critical properties at a DPT was presented by Park and Pleimling (Park & Pleimling, 2012). Both in two and three space dimensions they have obtained values for the surface critical exponents that differ markedly from the values of the equilibrium surface exponents, thus demonstrating that the dynamic surface universality class differs from that of the equilibrium system, even though the same universality class prevails for the corresponding bulk systems. However, the rich behavior depending on the dynamical parameters has not been covered in both works (Laosiritaworn, 2009; Park & Pleimling, 2012). Very recently, the effect of the random magnetic fields distributed by a Gaussian distribution centered at zero on the phase diagrams and ground state magnetization of the thin film was investigated by Akıncı (Akıncı, 2013).

In semi-infinite systems, depending on the ratio between surface and bulk exchange interactions, the system may order on the surface before it orders in the bulk which is called extraordinary transition. In the contrary of this, ordinary transition means that the surface critical temperature is the same as the bulk transition temperature. There exists a consensus in the literature that, the intersection point between these two transitions is called 'special point' (in other words 'crossover point') (Li & Baberschke, 1992; Binder & Hohenberg, 1974; Landau & Binder, 1990; Saber et al., 1999; Laosiritaworn et al., 2004; Cossio et al., 2006; Park & Pleimling, 2012; Akıncı, 2013; Zaim et al., 2008; Kaneyoshi et al., 1983). As the film gets thicker, it approaches the semi-infinite system, and this unusual effect shows itself as an intersection point in the phase diagrams plotted in critical temperature versus surface exchange interaction plane for the films with different thicknesses.

CHAPTER TWO
NONEQUILIBRIUM DYNAMICAL PHASE TRANSITIONS

In this chapter we will introduce and motivate the theoretical background we use. It will not exhaustively cover all details of the methods and systems under consideration, rather we will try to pedagogically introduce the extensions necessary for our calculations. A widely detailed description of the ideas given in here can be found in (Yeomans, 1993).

2.1 The Main Idea Behind Order-Disorder Transition

Order-disorder transition is one of the most important problem of equilibrium statistical mechanics (Reichl, 1997). The N identical spin-1/2 particle with the magnetic moment μ spin-1/2 system can be given as a simple example for such a problem. The magnetic item in any lattice site interacts with its nearest-neighbor induced magnetic field and external effect, i.e. magnetic field. The Hamiltonian for this type of system can be written as follow

$$\mathcal{H} = -\sum_{\langle ij \rangle} J_{ij} s_i s_j - H \sum_{i=1}^{N} s_i \tag{2.1}$$

where $H = \mu B$. The bra-kets in the first summation stands for nearest-neighboring. J_{ij} is the magnetic exchange interaction between the lattice sites, s_i is the z-component of the spin located in the ith lattice site, and last, B is the external magnetic field. For the spin-1/2 system the possible two values of the s_i (microstates in usual canonical ensemble) is ± 1. The Hamiltonian in Eqn. (2.1) contains only the information about the spin orientations and the spatial configuration of lattice sites. The ground state configuration of the system determines mainly by the sign of the exchange interaction. If J_{ij} is uniform and positive, namely $J_{ij} = J > 0$, hence all the spins will have a tendency to be the same direction to minimize the energy at zero temperature in the absence of external field. This is ordered phase called ferromagnetism. The reverse is valid and that is also an ordered phase which is called anti-ferromagnetism. The competition takes place between external field and thermal agitations. The partition

function for such a simple system can written as

$$\mathcal{Z}_N(T) = \sum_{\{s_i=\pm 1\}} \exp\left[-\beta \sum_{\langle ij \rangle} J_{ij} s_i s_j + \beta\mu B \sum_{i=1}^{N} s_i\right]. \tag{2.2}$$

Here argument of the first summation is all different configuration. As mentioned above, the exchange interaction generally forces the spins to be ordered. Contrary to this, thermal energy tends to this order. This competition is the core of order-disorder phase transitions. The Hamiltonian in Eqn. (2.1) has been first propounded by Ising to investigate to behavior ferromagnets (Ising, 1925). At the same time, the model has been also very successful to explain the lattice gas behavior (Mahan & Francisco, 1977), binary alloys (Upton & Yeomans, 1989) and the structure of the DNA (Etchegoin & Nöllmann, 2003).

There are exact solution of this model in one- and two-dimension. However, the three dimensional version of it has not been exactly solved yet.[1] The Ising model does not present ant phase transition at finite temperature in one-dimension. In one-dimension, any lattice site has not enough neighbors to compete with thermal energy. In higher-dimensions, this problem automatically will be removed. Two-dimensional Ising model has solved exactly by Onsager (Onsager, 1944; Kaufman & Onsager, 1949). This model is one of the rare exactly solvable models that shows phase transition.

2.2 Exact Solution of Equilibrium One-Dimensional Ising Model

The main idea is to write down the partition function in terms of a matrix, the transfer matrix. The thermodynamic properties of the model are then wholly described by the eigenspectrum of the matrix. In particular the free energy per spin in the thermodynamic limit depends only on the largest eigenvalue and the correlation length only on the two largest eigenvalues through simple formulae.

The simplest application of the transfer matrix technique is to the exact solution of

[1] As an academic issue, three-dimensional proof for Ising model impossible, Sandia researcher Sorin Istrail claims to have shown. *Sandia LabNews* Vol. 52, No. 8 (2000).

one-dimensional spin models with a finite number of neighbors per site and a finite number of spin states. Transfer matrices have, however, also proved very useful in the solution of exactly solvable two-dimensional models; now the matrices are infinite-dimensional and their analysis requires sophisticated mathematics (Baxter, 1982).

We shall now use the one-dimensional Ising model in a static magnetic field to setting up the the transfer matrix. The model is described by the Hamiltonian

$$\mathcal{H}_N = -J \sum_{i=0}^{N-1} s_i s_{i+1} - H \sum_{i=0}^{N-1} s_i \tag{2.3}$$

where we shall, for convenience, take periodic boundary conditions, that is identify $s_N \equiv s_0$. The choice of boundary conditions becomes irrelevant in the thermodynamic limit, $N \to \infty$.

The partition function, written out in some detail, is

$$\mathcal{Z} = \sum_{\{s\}} e^{\beta J(s_0 s_1 + s_1 s_2 + \ldots + s_{N-1} s_0) + \beta H(s_0 + s_1 + \ldots + s_{N-1})} \tag{2.4}$$

where $\{s\}$ represents the trace over all possible states of the system, that is the sum over $s_i = \pm 1$ for all spins s_i. The important property of Eqn. (2.4) that allows it to be represented as a product of matrices is that it can be rearranged into products of terms each depending only on nearest neighbor pairs

$$\begin{aligned} \mathcal{Z} &= \sum_{\{s\}} e^{\beta J s_0 s_1 + \beta H(s_0+s_1)/2} e^{\beta J s_1 s_2 + \beta H(s_1+s_2)/2} \ldots e^{\beta J s_{N-1} s_0 + \beta H(s_{N-1}+s_0)/2} && (2.5) \\ &\equiv \sum_{\{s\}} \mathbf{T}_{0,1} \mathbf{T}_{1,2} \ldots \mathbf{T}_{N-1,0} && (2.6) \end{aligned}$$

where

$$\mathbf{T}_{i,i+1} = e^{\beta s_i s_{i+1} + \beta H(s_i + s_{i+1})/2} \tag{2.7}$$

are the elements of a matrix $\mathbf{T}$ with rows labelled by the values of s_i and columns by

the values of s_{i+1}. Writing out $\mathbf{T}$ explicitly for the model we are considering

$$\begin{array}{c} \\ s_i = 1 \\ s_i = -1 \end{array} \begin{array}{c} \begin{array}{cc} s_{i+1} = 1 & s_{i+1} = -1 \end{array} \\ \begin{pmatrix} e^{\beta(J+H)} & e^{-\beta J} \\ e^{-\beta J} & e^{\beta(J-H)} \end{pmatrix} \end{array} \tag{2.8}$$

Eqn. (2.4) is easily simplified by nothing that it is a matrix product written in terms of the components of the matrix $\mathbf{T}$. Taking the trace over spins $i = 1, 2, \ldots, N-1$ corresponds to performing the product

$$\mathcal{Z}_N = \sum_{s_0 = \pm 1} (\mathbf{T}^N)_{0,0} \tag{2.9}$$

so that only the summation over s_0 of the diagonal elements of $\mathbf{T}^N$ remains. This is just the trace of $\mathbf{T}^N$ which is most usefully expressed in terms of the eigenvalues λ_i of $\mathbf{T}$

$$\mathcal{Z}_N = \sum_i \lambda_i^N . \tag{2.10}$$

Although we have used the example of the one-dimensional Ising model to enable us to display an explicit formula at each step, Eqn. (2.10) is a general result.

The transfer matrix method is useful whenever the partition function can be factorized in a form like Eqn. (2.3) and hence expressed as a product of matrices. A common application is to one-dimensional classical spin systems with finite-range interactions. The size of the transfer matrix depends on the number of spin states per site and on the range of the interactions. For example, for the nearest neighbor q-state Potts model it is $q \times q$. For the one-dimensional Ising model with first and second neighbor interactions the rows and columns are labelled by s_i, s_{i+1} and s_{i+2}, s_{i+3} respectively and hence the matrix is 4×4. As the model gets more complicated the usefulness of the formalism depends on whether the transfer matrix can be diagonalized analytically or numerically.

A pictorial way of thinking of the transfer matrix is that it builds up the lattice step

by step. Multiplying by the R^{th} power of $\mathbf{T}$ adds the spin s_R and traces over the spin s_{R-1}. Hence this step can be considered to add the bond between spins $R-1$ and R. Any further terms in $\mathcal{Z}$ cannot depend on the value of s_{R-1} as the trace has already been taken over this spin.

The power of the transfer matrix formalism becomes apparent in the formula for the free energy. We shall now leave the example of the Ising model and consider a general transfer matrix $\mathbf{T}$ of size $n \times n$. If the eigenvalues, listed in terms of decreasing modulus, are labelled $\lambda_0, \lambda_1, \lambda_2, \ldots, \lambda_{n-1}$ then, in the thermodynamic limit, the free energy per spin is given by

$$f = -k_B T \lim_{N\to\infty} \frac{1}{N} \ln \mathcal{Z}_N \tag{2.11}$$

$$= -k_B T \lim_{N\to\infty} \frac{1}{N} \ln \left\{ \lambda_0^N \left(1 + \sum_i \frac{\lambda_i^N}{\lambda_0^N} \right) \right\}. \tag{2.12}$$

But, as $N \to \infty$, $(\lambda_i/\lambda_0)^N \to 0$ because the ratio is less than 1 and hence

$$f = -k_B T \ln \lambda_0. \tag{2.13}$$

This is an important result because it is often much easier to calculate λ_0 than the entire spectrum of a matrix.

It is not necessary to worry about degeneracy in λ_0 because transfer matrices can be proved to belong to a class of matrices with non-degenerate, positive largest eigenvalue λ_0, thus giving a physically sensible free energy.[2] We have assumed that the λ_i are real. This is not necessarily the case for $i \neq 0$ but the formula Eqn. (2.13) still holds.

A second important quantity which is simply related to the eigenvalues of the transfer matrix is the correlation length. To calculate this we need the spin-spin correlation function which serves as an example of how to obtain averages of products of spins using transfer matrices. The usual definitions of Γ_R, the two-spin correlation

[2]This is the Perron-Frobenius theorem which is discussed in Horn, R. A. and Johnson, C. A. (1985). *Matrix analysis*, p.508. (Cambridge University Press, Cambridge).

function, and ξ, the correlation length,

$$\Gamma_R = (\langle s_0 s_R\rangle - \langle s_0\rangle\langle s_R\rangle), \tag{2.14}$$

$$\xi^{-1} = \lim_{R\to\infty}\left\{-\frac{1}{R}\ln|\langle s_0 s_R\rangle - \langle s_0\rangle\langle s_R\rangle\right\}. \tag{2.15}$$

Consider first the calculation of

$$\langle s_0 s_R\rangle_N = \frac{\sum_{\{s\}} s_0 s_R e^{-\beta\mathcal{H}_N}}{\sum_{\{s\}} e^{-\beta\mathcal{H}_N}} \equiv \frac{1}{\mathcal{Z}_N}\sum_{\{s\}} s_0 s_R e^{-\beta\mathcal{H}_N} \tag{2.16}$$

where the subscript N denotes that we are again considering a ring of N spins. $\mathcal{Z}_N$ is known from Eqn. (2.10) and the numerator can be written in a form analogous to Eqn. (2.4)

$$\begin{aligned}\sum_{\{s\}} s_0 s_R e^{-\beta\mathcal{H}_N} &= \sum_{\{s\}} \varepsilon_0 \mathbf{T}_{0,1}\mathbf{T}_{1,2}\ldots\mathbf{T}_{R-1,R}s_R\mathbf{T}_{R,R+1}\ldots\mathbf{T}_{N-1,0}\\ &= \sum_{s_0 s_R} s_0(\mathbf{T}^R)_{0,R}s_R(\mathbf{T}^{N-R})_{R,0}.\end{aligned} \tag{2.17}$$

Let T have eigenvectors $|\vec{u}_i\rangle$ corresponding to the eigenvalues λ_i, $i = 0,1,2,\ldots,n-1$. It will also be useful to define the diagonal matrix s_R with eigenvalues equal to the possible values of s_R and corresponding eigenvectors $\langle\vec{S}_R| = (00\ldots010\ldots00)$. Making use of the formulae

$$s_R = \sum_{s_R} |\vec{s}_R\rangle s_R\langle\vec{s}_R|, \tag{2.18}$$

$$\mathbf{T} = \sum_i |\vec{u}_i\rangle\lambda_i\langle\vec{u}_i|, \tag{2.19}$$

and

$$(\mathbf{T}^R)_{0,R} = \sum_i \langle\vec{s}_0|\vec{u}_i\rangle\lambda_i^R\langle\vec{u}_i|\vec{s}_R\rangle \tag{2.20}$$

Eqn. (2.17) becomes

$$\sum_{\{s\}} s_0 s_R e^{-\beta\mathcal{H}_N} = \sum_{s_0 s_R}\sum_{i,j} s_0\langle\vec{s}_0|\vec{u}_i\rangle\lambda_i^R\langle\vec{u}_i|\vec{s}_R\rangle s_R\langle\vec{s}_R|\vec{u}_j\rangle\lambda_j^{N-R}\langle\vec{u}_j|\vec{s}_0\rangle. \tag{2.21}$$

Moving the final matrix element to the beginning of the product and using Eqn. (2.18):

$$\sum_{\{s\}} s_0 s_R e^{-\beta \mathcal{H}_N} = \sum_{i,j} \langle \vec{u}_j | s_0 | \vec{u}_i \rangle \lambda_i^R \langle \vec{u}_i | s_R | \vec{u}_j \rangle \lambda_j^{N-R}. \tag{2.22}$$

Hence, recalling the formula (2.10) for $\mathcal{Z}$,

$$\langle s_0 s_R \rangle_N = \frac{\sum_{i,j} \langle \vec{u}_j | s_0 | \vec{u}_i \rangle \left(\frac{\lambda_i}{\lambda_0}\right)^R \langle \vec{u}_i | s_R | \vec{u}_j \rangle \left(\frac{\lambda_i}{\lambda_0}\right)^{N-R}}{\sum_k \left(\frac{\lambda_k}{\lambda_0}\right)^N} \tag{2.23}$$

where we have divided through by λ_0. It is then easy to see that in the thermodynamic limit only the terms in $j = 0$ and $k = 0$ survive

$$\begin{aligned} \langle s_0 s_R \rangle &= \lim_{N\to\infty} \langle s_0 s_R \rangle_N = \sum_i \left(\frac{\lambda_i}{\lambda_0}\right)^R \langle \vec{u}_0 | s_0 | \vec{u}_i \rangle \langle \vec{u}_i | s_R | \vec{u}_0 \rangle & (2.24) \\ &= \langle \vec{u}_0 | s_0 | \vec{u}_0 \rangle \langle \vec{u}_0 | s_R | \vec{u}_0 \rangle + \sum_{i\neq 0} \left(\frac{\lambda_i}{\lambda_0}\right)^R \langle \vec{u}_0 | s_0 | \vec{u}_i \rangle \langle \vec{u}_i | s_R | \vec{u}_0 \rangle \\ &= \langle s_0 \rangle \langle s_R \rangle + \sum_{i\neq 0} \left(\frac{\lambda_i}{\lambda_0}\right)^R \langle \vec{u}_0 | s_0 | \vec{u}_i \rangle \langle \vec{u}_i | s_R | \vec{u}_0 \rangle & (2.25) \end{aligned}$$

where in the final step we have used

$$\langle s_R \rangle = \langle \vec{u}_0 | s_R | \vec{u}_0 \rangle \tag{2.26}$$

which can be proved by a method entirely analogous to that followed above.

The correlation function (2.14) then follows immediately as

$$\Gamma_R = \sum_{i\neq 0} \left(\frac{\lambda_i}{\lambda_0}\right)^R \langle \vec{u}_0 | s_0 | \vec{u}_i \rangle \langle \vec{u}_i | s_R | \vec{u}_0 \rangle. \tag{2.27}$$

Note that it depends on all the eigenvalues and eigenvectors of the transfer matrix. A much simpler formula is obtained for the correlation length (2.15). Taking the limit

$R \to \infty$ the term $i = 1$ dominates the sum in Eqn. (2.27) and hence

$$\xi^{-1} = \lim_{R\to\infty} -\frac{1}{R} \ln\left\{\left(\frac{\lambda_1}{\lambda_0}\right)^R \langle\vec{u}_0|s_0|\vec{u}_1\rangle\langle\vec{u}_1|s_R|\vec{u}_0\rangle\right\} \tag{2.28}$$

$$= -\ln(\lambda_1/\lambda_0). \tag{2.29}$$

This formula has proved invaluable in work involving large transfer matrices it is far easier numerically to find a small number of dominant eigenvalues than to completely diagonalize the matrix.

A point worth noting is that usually the Hamiltonian considered is translationally invariant. Hence the product of matrix elements in Eqn. (2.27) can be rewritten

$$\langle\vec{u}_0|s_0|\vec{u}_i\rangle\langle\vec{u}_i|s_R|\vec{u}_0\rangle = |\langle\vec{u}_i|s_0|\vec{u}_0\rangle|^2. \tag{2.30}$$

We have also ignored the possibility that λ_i, $i \neq 0$, can be complex.

Let us now return to the nearest-neighbor Ising model in a magnetic field, to obtain the explicit results for the quantities discussed above. Diagonalizing the matrix (2.8) gives

$$\lambda_{0,1} = e^{\beta J}\cosh(\beta J)\cosh(\beta H) \pm \sqrt{e^{2\beta J}\sinh^2(\beta H) + e^{-2\beta J}} \tag{2.31}$$

$$\langle\vec{u}_0| = (\alpha_+, \alpha_-), \qquad \langle\vec{u}_1| = (\alpha_-, -\alpha_+) \tag{2.32}$$

where

$$\alpha_\pm^2 = \frac{1}{2}\left(1 \pm \frac{e^{\beta J}\sinh(\beta H)}{\sqrt{e^{2\beta J}\sinh^2(\beta H)e^{-2\beta J}}}\right). \tag{2.33}$$

Using Eqns. (2.31)-(2.33) we shall write down expressions for the free energy per spin f, the magnetization per spin $\langle s\rangle$, the correlation function Γ, and the correlation length ξ, and check that they behave in a sensible way.

From Eqns. (2.13)-(2.31)

$$f = -k_B T \ln\left\{e^{\beta J}\cosh(\beta H) + \sqrt{e^{2\beta J}\sinh^2(\beta H) + e^{-2\beta J}}\right\}. \tag{2.34}$$

As $\beta \to \infty$

$$f \to -k_B T \ln\{e^{\beta J}(\cosh(\beta H) + \sinh(\beta H))\} = -J - H \tag{2.35}$$

which is the energy per spin as expected.

Also the magnetization can be obtained either by differentiating the negative of the free energy with respect to the magnetic field H. One obtains

$$\langle s \rangle = (\alpha_+, \alpha_-)\begin{pmatrix} 1 & 0 \\ 0 & -1 \end{pmatrix}\begin{pmatrix} \alpha_+ \\ \alpha_- \end{pmatrix} \tag{2.36}$$

$$= \frac{e^{\beta J}\sinh(\beta H)}{\sqrt{e^{2\beta J}\sinh^2(\beta H) + e^{-2\beta J}}}. \tag{2.37}$$

For non-interacting spins $J = 0$ (or equivalently $T = \infty$), this reduces to

$$\langle s \rangle = \tanh(\beta H) \tag{2.38}$$

as expected for a paramagnet. In zero field at any finite temperature $\langle s \rangle = 0$, as expected from the symmetry of the model, unless one takes the temperature to zero with H finite and then the field to zero

$$\lim_{H \to 0^{\pm}} \lim_{T \to 0} \langle s \rangle = \pm 1 \tag{2.39}$$

showing that there is a phase transition at zero temperature to a fully ordered ground state. From Eqn. (2.27)

$$\Gamma_R = \frac{\lambda_1}{\lambda_0}^R \frac{e^{-2\beta J}}{e^{2\beta J}\sinh^2(\beta H) + e^{-2\beta J}}. \tag{2.40}$$

From zero field this simplifies to

$$\Gamma_R(H = 0) = \tanh^R(\beta J). \tag{2.41}$$

The zero-field correlation function is plotted as a function of R for different temperatures in Fig. 2.1. Note the expected decay with R for all $T \neq 0$. If the coupling is antiferromagnetic ($J < 0$) the correlation function changes sign for odd R.

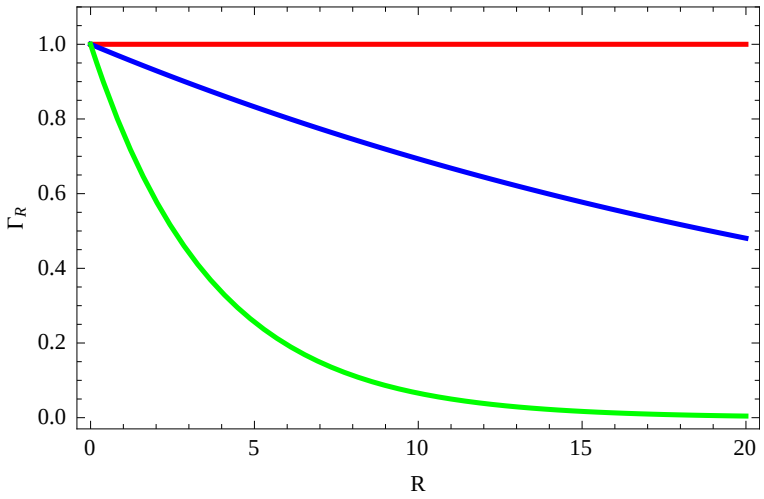

Figure 2.1 Dependence of the spin-spin correlation function of the one-dimensional Ising model in zero field on distance and temperature. Red, blue and green lines correspond to the different temperatures as $k_B T/J = 0$, 0.5, and 1.0 respectively.

From Eqn. (2.29)

$$\xi^{-1} = \ln\left\{\frac{e^{\beta J}\cosh(\beta H) - \sqrt{e^{2\beta J}\sinh^2(\beta H) + e^{-2\beta J}}}{e^{\beta J}\cosh(\beta H) + \sqrt{e^{2\beta J}\sinh^2(\beta H) + e^{-2\beta J}}}\right\}. \tag{2.42}$$

Check that as $T \to 0$, $\xi^{-1} \to 0$ signalling the expected phase transition and that as $T \to \infty$, $\xi^{-1} \to \infty$.

2.3 Mean-Field Approximation for The Ising Model in d-Dimension

Very few models statistical mechanical models have been solved exactly. In three dimensions not even the nearest-neighbor spin-1/2 Ising model is tractable. Therefore it is necessary to resort to approximation methods. One of the most widely used of these is mean-field theory.

A systematic way of deriving the mean-field theory for a given microscopic Hamiltonian is to start from Bogoliubov inequality[3]

$$\mathcal{F} \leq \Phi = \mathcal{F}_0 + \langle \mathcal{H} - \mathcal{H}_0 \rangle_0 \tag{2.43}$$

[3]A proof is given in Callen, H. B. (1985). *Thermodynamics and an introduction to thermostatistics* (2nd edn.), p.433 (Wiley, New York).

where $\mathcal{F}$ is the true free energy of the system, $\mathcal{H}_0$ a trial Hamiltonian depending on a parameter $\mathcal{H}_0$, $\mathcal{F}_0$ the corresponding free energy, and $\langle \ldots \rangle_0$ denotes an average taken in the ensemble defined by $\mathcal{H}_0$.

The mean-field free energy is then defined by minimizing Φ with respect to the variational parameter $\mathcal{H}_0$

$$\mathcal{F}_{\rm mf} = \min_{H_0}\{\Phi\}. \tag{2.44}$$

This gives the best possible approximation to the true free energy for a given choice of $\mathcal{H}_0$ because the inequality (2.43) insists that the mean-field free energy cannot fall below the true free energy. (This is analogous to the variational principle in quantum mechanics.) The usual choice for $\min_{H_0}$ is a free Hamiltonian - one with no interactions - as this enables explicit calculation of the right-hand side of (2.43).

As an example we consider the nearest-neighbor Ising model in zero field, defined by the Hamiltonian (2.45) with $H = 0$, on a lattice of N sites with each site having z nearest-neighbors. For the simple cubic lattice $z = 6$. The trial Hamiltonian is

$$\mathcal{H}_0 = -H_0 \sum_i s_i, \tag{2.45}$$

where H_0 is termed the mean field.

This is just the Hamiltonian of a paramagnet. Therefore

$$\mathcal{F}_0 = -Nk_BT \ln(2\cosh(\beta H_0)), \tag{2.46}$$

$$\langle s \rangle_0 = \tanh(\beta H_0). \tag{2.47}$$

We also need

$$\begin{aligned} \langle \mathcal{H} - \mathcal{H}_0 \rangle_0 &= \frac{\sum_{\{s\}}(-J\sum_{\langle ij\rangle} s_i s_j + H_0 \sum_i s_i)\exp[\beta H_0 \sum_i s_i]}{\sum_{\{ij\}} \exp[\beta H_0 \sum_i s_i]} \\ &= -J\sum_{\langle ij\rangle} \langle s_i\rangle_0 \langle s_j\rangle_0 + H_0 \sum_i \langle s_i\rangle_0 \end{aligned} \tag{2.48}$$

where the factorization of the interaction term is possible because $\mathcal{H}_0$ contains only single-site terms. For a translationally invariant system $\langle s_i\rangle_0 = \langle s_j\rangle_0 \equiv \langle s_0\rangle$ and the sums can be performed to give

$$\langle \mathcal{H} - \mathcal{H}_0\rangle_0 = -JzN\langle s\rangle_0^2/2 + NH_0\langle s\rangle_0 \tag{2.49}$$

where $zN/2$ is the number of bonds on the lattice ('each of N sites has z bonds each of which is shared between two neighbors!'). Substituting Eqns. (2.46) and (2.49) into (2.43) and using Eqn. (2.47) one obtains

$$\Phi = -Nk_BT\ln(2\cosh(\beta H_0)) - \frac{JzN}{2}\tanh^2(\beta H_0) - NH_0\tanh(\beta H_0). \tag{2.50}$$

Minimizing this expression with respect to H_0 gives a self-consistent expression for the mean field

$$H_0 = Jz\tanh(\beta H_0) \tag{2.51}$$

or equivalently, noting from Eqn. (2.47) that $H_0 = Jz\langle s\rangle_0$, for the mean-field magnetization

$$\langle s\rangle_0 = \tanh(\beta Jz\langle s\rangle_0). \tag{2.52}$$

Substituting Eqn. (2.51) back into Eqn. (2.50) shows that the mean-field free energy is

$$\mathcal{F}_{\rm mf} = -Nk_BT\ln(2\cosh(\beta Jz\langle s\rangle_0)) + NJz\langle s\rangle_0^2/2. \tag{2.53}$$

To obtain the temperature dependence of the mean-field magnetization we need to solve Eqn. (2.52). The easiest way to obtain a qualitative understanding of how this behaves is to plot $\langle s\rangle_0$ for different values of the temperature. This is done in Fig. 2.2(a). The intersections of the curves correspond to values of $\langle s\rangle_0$ which solve Eqn. (2.42).

For temperatures greater than some value T_c, the only solution is $\langle s\rangle_0 = 0$ corresponding to the paramagnetic phase, whereas, for temperatures less than T_c, there

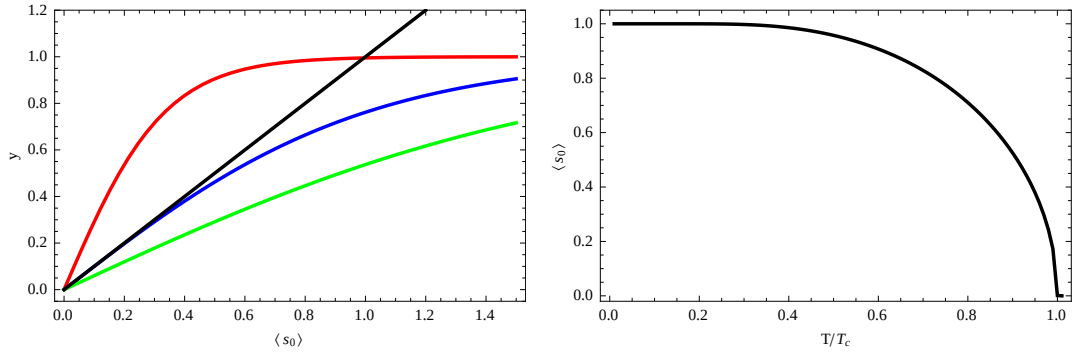

(a) (b)

Figure 2.2 (a) Graphical solution of the equation for the mean-field magnetization. Red, blue and green lines correspond to the different temperatures as $T < T_c$, $T = T_c$, and $T > T_c$ respectively. $y = \langle s \rangle_0$ line stands for the visual clarity about critical temperature. (b) Temperature dependence of the mean-field magnetization.

are two solutions, $\langle s \rangle_0 = 0$ and a finite value of $\langle s \rangle_0$. One can check that the former corresponds to a maximum and the latter to a minimum of the mean-field free energy (2.53). Hence the stable phase is ferromagnetic. It is evident from Fig. 2.2(a) that the transition temperature T_c is calculated by equating the gradients of the two curves $\langle s \rangle_0$ and $\tanh(\beta J z \langle s \rangle_0)$ at the origin. This gives

$$k_B T_c = Jz. \tag{2.54}$$

Note that T_c depends only on z, the number of nearest-neighbors, not on the other details of the lattice structure such as the dimensionality. One consequence of this is that the mean-field theory incorrectly predicts a finite temperature phase transition for the one-dimensional Ising model.

Following the ferromagnetic solution as the temperature is decreased from T_c it is apparent from Fig. 2.2(a) that $\langle s \rangle_0$ increases continuously from zero and therefore that the phase transition is continuous. As the temperature tends to zero, $\langle s \rangle_0 \to 1$, because the tanh is bounded by unity. Physically this corresponds as expected to all the spins becoming aligned. $\langle s \rangle_0$ is plotted as a function of temperature in Fig. 2.2(b).

2.3.1 Landau Theory

Landau theory is based on very simple assumptions, yet it not only predicts a phase transition but allows reproduction of the mean-field exponents showing very clearly how they depend on the symmetry of the order parameter. Landau assumed that the free energy can be expanded as a power series in the order parameter m where only those terms compatible with the symmetry of the system are included.

For example, for a simple ferromagnet in zero external field,

$$\mathcal{F} = \mathcal{F}_0 + a_2 m^2 + a_4 m^4 \tag{2.55}$$

because only even terms are invariant under a reversal in the sign of the magnetization. The series can be truncated after the term $O(m^4)$ because, as we shall see, if a_4 is taken to be positive, subsequent terms cannot after the critical behavior of the system.

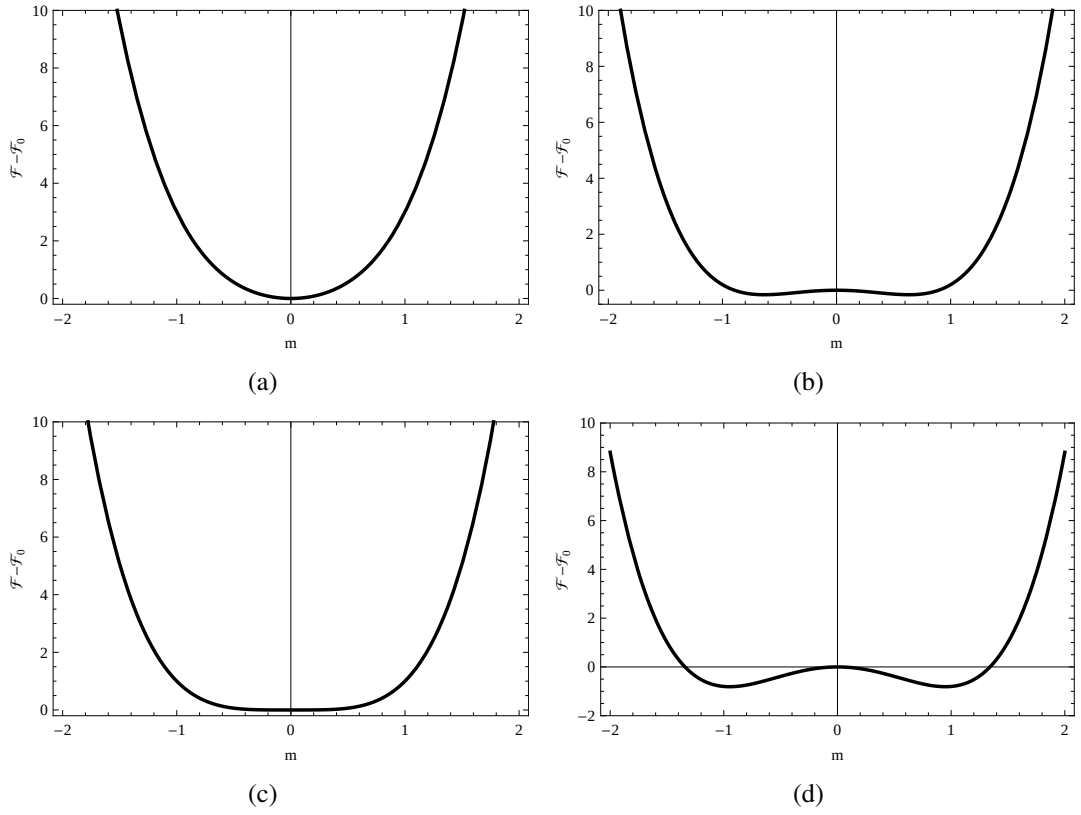

Figure 2.3 Variation of the Landau free energy with magnetization for decreasing values of a_2. (a) $a_2 > 0$, (b) $a_2 = 0$ (c) $a_2 \simeq 0$, (d) $a_2 < 0$.

The Landau free energy is plotted as a function of m for decreasing values of a_2 in Fig. 2.3(a)-2.3(d). For $a_2 > 0$ the minimum value of $\mathcal{F}$ occurs at $m = 0$ showing that the system is in the paramagnetic phase. For $a_2 < 0$, however, the minimum free energy corresponds to a finite value of the order parameter m_0, indicating a ferromagnetic phase. Two stable states with magnetizations $+m_0$ and $-m_0$ coexist as a consequence of the physical symmetry built into $\mathcal{F}$. $a_2 = 0$ corresponds to the critical temperature where a spontaneous magnetization appears. Hence we may write,

$$a_2 = \tilde{a}_2 t \tag{2.56}$$

where t is the reduced temperature. Note that taking $a_4 > 0$ corresponds to the physical condition that the magnetization must be bounded.

It is at first sight surprising that singular behavior can be obtained from a regular expansion. This happens because the value of the magnetization which minimizes the free energy is itself a singular function of the expansion coefficients which depend on the field and temperature. What is the order of the transition? Consideration of the shape of the free energy curve as a_2 decreases from zero (Fig. 2.3(c) and 2.3(d)) shows that the magnetization becomes non-zero continuously but with a discontinuous derivative.

2.3.2 The Correlation Function

To obtain the mean-field values of the related exponents which describe the behavior of the correlation function we need to invoke the Ornstein-Zernike extension to Landau theory. This allows the magnetization to vary with position. We define a magnetization density $m(\vec{r})$ where $\vec{r}$ is a d-dimensional vector. To lowest order

$$\mathcal{F} - \mathcal{F}_0 = \tilde{a}_2^{\dagger} \int \{m(\vec{r})\}^2 d^d\vec{r} + g \int \{\nabla m(\vec{r})\}^2 d^d\vec{r}. \tag{2.57}$$

The first term on right-hand side is just the quadratic term in Eqn. (2.57) written as an integral over d-dimensional space to allow for the $\vec{r}$−dependence of the magnetization. The second term is lowest order term in the expansion of the spin-spin interaction and

takes into account the extra free energy that results if the spins are not parallel.

The results we need can be obtained by working in Fourier space because, within the Ornstein-Zernike approximation, the modes corresponding to different wavevectors are independent or one another. The Fourier transform of $m(\vec{r})$, $m(\vec{q})$, is defined by

$$m(\vec{r}) = \frac{1}{(2\pi)}^{d} \int d^d\vec{q} e^{i\vec{q}\vec{r}} \tilde{m}(\vec{q}), \tag{2.58}$$

$$m(\vec{q}) = \int d^d\vec{r} e^{-i\vec{q}\vec{r}} m(\vec{r}). \tag{2.59}$$

Remembering that

$$\int d^d\vec{r} e^{-i\vec{q}\vec{r}} = (2\pi)^d \delta(\vec{q}) \tag{2.60}$$

and that, because $m(\vec{r})$ is real, $\tilde{m}^*(\vec{q}) = m(\tilde{-}\vec{q})$ Eqn. (2.58) can be used to rewrite Eqn. (2.57) as

$$\mathcal{F} - \mathcal{F}_0 = \int \frac{d^d\vec{q}}{(2\Pi)^d} (\tilde{a}_2 tgq^2) |\tilde{m}(\vec{q})|^2. \tag{2.61}$$

Eqn. (2.61) displays the free energy as a sum of quadratic terms, each of which, by equipartition of energy, contributes an average of $k_B T$

$$(\tilde{a}_2 t + gq^2)\langle|\tilde{n}(\vec{q})|\rangle = k_B T. \tag{2.62}$$

The next step is to see how $\langle|\tilde{n}(\vec{q})|\rangle$ is related to the correlation function. This is defined for discrete spins and we shall need the obvious generalization to continuous variables

$$\Gamma(\vec{r}) = \langle m(\vec{r}) m(\vec{0})\rangle - \langle m(\vec{0})\rangle^2. \tag{2.63}$$

Taking the Fourier transform of Eqn. (2.63) by using Eqn. (2.58) and (2.59), and

considering the paramagnetic phase[4] so that $\langle m(\vec{0})\rangle = 0$

$$\Gamma(\vec{r}) = \langle \vec{m}(\vec{q}) m(\vec{0})\rangle \tag{2.64}$$

$$= \int \frac{d^d\vec{q}'}{(2\pi)^d} \langle \tilde{m}(\vec{q})\tilde{m}(\vec{q}')\rangle \tag{2.65}$$

where we have neglected the $\vec{r}$-independent term. Because the different modes are uncorrelated

$$\langle \tilde{m}(\vec{q})\tilde{m}(\vec{q}')\rangle = \delta(\vec{q}+\vec{q}')(2\pi)^d \langle |\tilde{m}(\vec{q})|^2\rangle. \tag{2.66}$$

Using Eqn. (2.66) in Eqn. (2.65) the formula simplifies considerably to give

$$\tilde{\Gamma}(\vec{q}) = \langle |\tilde{m}(\vec{q})|^2\rangle. \tag{2.67}$$

Substituting Eqn. (2.62) into Eqn. (2.67) immediately gives an expression for the Fourier transform of the pair correlation function.

$$\tilde{\Gamma}(\vec{q}) = \frac{k_B T}{\tilde{a}_2 t + g q^2}. \tag{2.68}$$

Taking the inverse transform

$$\Gamma(\vec{r}) \qquad \frac{e^{-r/\xi}}{r^{d-3}/2}, \quad t \neq 0 \tag{2.69}$$

$$\Gamma(\vec{r}) \qquad \frac{1}{r^{d-2}}, \quad t = 0. \tag{2.70}$$

2.3.3 Classical Mean-Field Theories

Landau theory unifies a number of early theories of phase transitions which are now recognised as mean-field theories. These may well be familiar. We now consider a magnetic system: Weiss theory of magnetism which is the first theory of an interacting magnetic system was due to Weiss in 1907. He argued that the effects of cooperative ordering can be mimicked by assuming that each spin is subject to an effective field

[4]The same exponents are obtained, as expected, for $T < T_c$. See Huang, K. (1987). *Statistical mechanics* (2nd edn.), p.425. (Wiley, New York).

proportional to the magnetization. Hence in the usual equation for the magnetization of a paramagnet, the external field is supplemented by an internal field $\lambda\langle s\rangle_0$

$$\langle s\rangle_0 = \tanh(\beta(H + \lambda\langle s\rangle)_0) \tag{2.71}$$

where λ is a constant which is related to the critical temperature, T_c. The derivation of the mean-field equations presented here, which starts from the Bogoliubov inequality, has allowed us to express the mean-field parameter λ in terms of the microscopic interaction J.

2.4 Effective-Field Theory

It is well known that the EFT is one of the most powerful methods that determines the boundary which separates several phases in the relevant planes, based on the use of rigorous correlation identities as a starting point and utilizes the differential operator technique developed by Honmura and Kaneyoshi (Honmura & Kaneyoshi, 1979). Although the conventional version of the method fails to find an expression for the free energy, since it takes into account the self spin correlations, the method is superior to MFT which neglects the thermal fluctuations via neglecting the self spin correlations. Thus, it is expected from EFT to obtain more reasonable results than MFT, as in the case of static Ising model.

2.4.1 Differential Operator Technique and Equation of State

The starting point of EFT is to write down the thermal average of a spin in canonical ensemble. As noted by Kaneyoshi (Kaneyoshi, 1980), in the presence of extremely high anisotropic case, we can treat a spin model by considering only the z-component of a spin. Hence, we use the Ising model Hamiltonian of ferromagnetism given in Eq. (2.1).

$$m_i = \langle s_i\rangle = \frac{1}{\mathcal{Z}}\mathrm{Tr} s_i e^{-\beta\mathcal{H}}. \tag{2.72}$$

The contribution coming from selected spin,

$$\mathcal{H}_i = -s_i(E_i + H). \tag{2.73}$$

The commutation relation also is follows,

$$[s_i, s_j] = 0. \tag{2.74}$$

hence the average coming from the spin with the index i,

$$\langle s_i \rangle = \frac{1}{\mathcal{Z}} \left(\mathrm{Tr} e^{-\beta \mathcal{H}} \left(\frac{\mathrm{Tr}_i s_i e^{-\beta \mathcal{H}_i}}{\mathrm{Tr}_i e^{-\beta \mathcal{H}_i}} \right) \right). \tag{2.75}$$

By taking into consideration the two states of spin $s = \pm 1$, we can get the related traces,

$$\begin{aligned} s = 1 \quad &\Rightarrow \quad \mathcal{H}_1 = -\frac{E_i}{2} - \frac{H}{2}, \\ s = -1 \quad &\Rightarrow \quad \mathcal{H}_2 = \frac{E_i}{2} + \frac{H}{2}, \end{aligned} \tag{2.76}$$

then,

$$\langle s_i \rangle = \frac{1}{\mathcal{Z}} \mathrm{Tr} e^{-\beta \mathcal{H}} \left(\frac{\sum_{s_i=-1}^{1} e^{-\beta \mathcal{H}_i}}{\sum_{s_i=-1}^{1} e^{-\beta \mathcal{H}_i}} \right). \tag{2.77}$$

$$\langle s_i \rangle = \frac{1}{\mathcal{Z}} \frac{1}{2} \left(\mathrm{Tr} e^{-\beta \mathcal{H}} \left(\frac{e^{\frac{\beta}{2}(E_i+H)} - e^{\frac{-\beta}{2}(E_i+H)}}{e^{\frac{\beta}{2}(E_i+H)} + e^{\frac{-\beta}{2}(E_i+H)}} \right) \right), \tag{2.78}$$

$$\langle s_i \rangle = \frac{1}{\mathcal{Z}} \frac{1}{2} \left(\mathrm{Tr} e^{-\beta \mathcal{H}} \left(\frac{2 \sinh[\frac{\beta}{2}(E_i + H)]}{2 \cosh[\frac{\beta}{2}(E_i + H)]} \right) \right), \tag{2.79}$$

$$\langle s_i \rangle = \frac{1}{2} \frac{1}{\mathcal{Z}} \left(\mathrm{Tr} e^{-\beta \mathcal{H}} \tanh[\frac{\beta}{2}(E_i + H)] \right). \tag{2.80}$$

Finally we get,

$$\langle s_i \rangle = \frac{1}{2} \left\langle \tanh\left(\frac{\beta}{2}[E_i + H] \right) \right\rangle. \tag{2.81}$$

Eqn. (2.81) is called Callen Identity. Here, we apply differential operator technique. We consider an exponential operator as follows

$$e^{\alpha\nabla} f(x) = f(x+\alpha)|_{x=0} \tag{2.82}$$

where α is any real number and $\nabla = d/dx$. The series expansion of this,

$$\begin{aligned} e^{\alpha\nabla} f(x) &= \left[1 + \alpha\nabla + \frac{\alpha^2}{2!}\nabla^2 + \ldots\right] f(x), \\ &= f(x) + \alpha\nabla f(x) + \frac{\alpha^2}{2!}\nabla^2 f(x) \ldots = f(x+\alpha)|_{\alpha=0}. \end{aligned} \tag{2.83}$$

By using this identity, we get

$$\langle s_i \rangle = \frac{1}{2}\langle \tanh\left(\frac{\beta}{2}[E_i + H]\right)\rangle = \frac{1}{2}\langle e^{E_i\nabla} \tanh\left(\frac{\beta}{2}[x + H]\right)\rangle|_{x=0}. \tag{2.84}$$

Thus,

$$\langle s_i \rangle = \langle e^{E_i\nabla}\rangle F(x)|_{x=0} \tag{2.85}$$

where

$$F(x) = \frac{1}{2}\tanh\left(\frac{\beta}{2}[x + H]\right). \tag{2.86}$$

The energy contribution coming from *ith* spin,

$$E_i = J\sum_j s_j \tag{2.87}$$

Let us choose a single site and its neighbors in a cluster which represents the topology of the system as seen in Fig. 2.4.

$$\langle s_i \rangle = \langle e^{(J\sum_j s_j)\nabla}\rangle F(x)|_{x=0}, \tag{2.88}$$

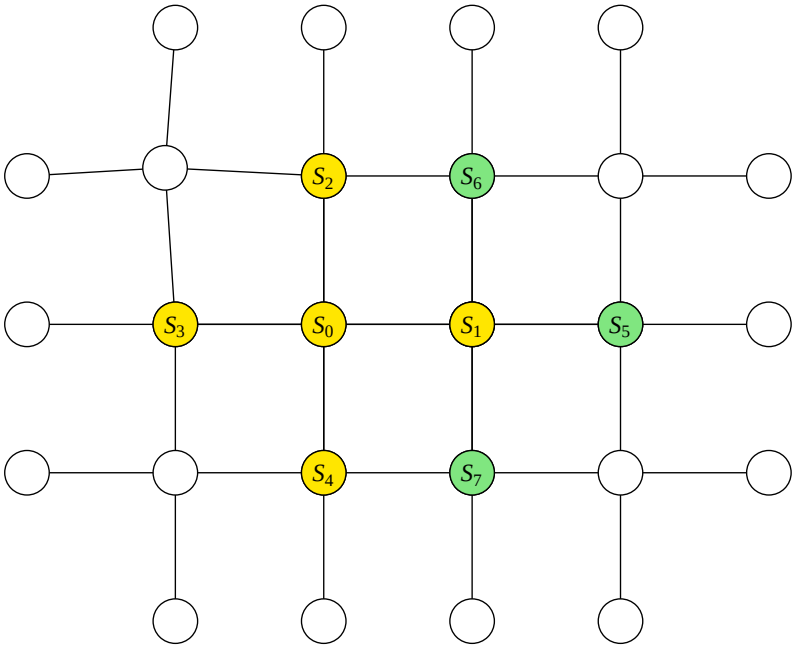

Figure 2.4 The interactions between central spin (s_0) and its nearest neighbors (s_1, s_2, s_3, s_4) are defined exactly. Also, an effective-field is needed generated from the interactions between s_1 and s_5, s_6, s_7.

$$\begin{aligned} s_0 &\rightarrow E_0, \\ s_\delta &\rightarrow E_\delta, \end{aligned} \tag{2.89}$$

As an example, the number of nearest neighbors in a square lattice $z = 4$. So,

$$\langle s_i \rangle = \left\langle e^{J \sum_{j=1}^{4} s_j \nabla} \right\rangle F(x)|_{x=0} \tag{2.90}$$

$$\begin{aligned} \langle s_0 \rangle &= \left\langle \prod_{j=1}^{4} e^{j s_j \nabla} \right\rangle F(x)|_{x=0}, \\ \langle s_1 \rangle &= \left\langle e^{(j s_0)+(q-1)A\nabla} \right\rangle F(x)|_{x=0} \end{aligned} \tag{2.91}$$

where $\gamma = (q-1)A$.

$$\langle s_1 \rangle = \left\langle e^{js_0\nabla} e^{\gamma\nabla} \right\rangle F(x)|_{x=0} = \left\langle e^{js_0\nabla} \right\rangle F(x+\gamma)|_{x=0} \tag{2.92}$$

where we use the identity $e^{\gamma\nabla} F(x)|_{x=0} = F(x+\gamma)|_{x=0}$.

By using the Van der Waerden identity for two-state spin, i.e., $\exp(bs_i) = \cosh(b) + s_i \sinh(b)$ where b is any real constant in a representative manner, we write the exponential terms in the thermal averages of central spin and its neighbor in terms of the hyperbolic trigonometric functions, hence we get the equations of state as follow.

$$\begin{aligned}
\langle s_0 \rangle &= \left\langle \prod_{j=1}^{4} \left(\cosh\left(\frac{J\nabla}{2}\right) + 2s_j \sinh\left(\frac{J\nabla}{2}\right) \right) \right\rangle F(x)|_{x=0}, \\
\langle s_1 \rangle &= \left\langle \cosh\left(\frac{J\nabla}{2}\right) + 2s_0 \sinh\left(\frac{J\nabla}{2}\right) \right\rangle F(x+\gamma)|_{x=0}.
\end{aligned} \tag{2.93}$$

2.4.2 Decoupling (Zernike) Approximation

Generalization of the Callen identity (2.81) as

$$\langle \{f_i\} s_i \rangle = \langle \{f_i\} \tanh(\beta E_i) \rangle, \tag{2.94}$$

where $\{f_i\}$ can be any function as long as it is not a function of the site i. By using differential operator technique and Van der Waerden identity in Eqn. (2.94) yields

$$\begin{aligned}
\langle \{f_i\} s_i \rangle &= \langle \{f_i\} e^{E_i\nabla} \tanh(\beta x) \rangle, \\
&= \langle \{f_i\} e^{\left(J\sum_j s_j + H\right)\nabla} \tanh(\beta x) \rangle, \\
&= \langle \{f_i\} \prod_j e^{Js_j\nabla} \tanh[\beta(x+H)] \rangle,
\end{aligned} \tag{2.95}$$

from which we finally obtain

$$\langle \{f_i\} s_i \rangle = \left\langle \{f_i\} \prod_{j=1}^{z} [\cos(J\nabla) + s_i \sinh(J\nabla)] \right\rangle f(x)|_{x=0}, \tag{2.96}$$

where

$$f(x) = \tanh[\beta(x+H)]. \tag{2.97}$$

When we expand right-hand side of Eqn.(2.96) thermal averages of multiple correlation functions occur. In order to overcome this equation solvable one has to make an approximation. The simplest approximation, and one of the most frequently adopted, is to decouple these correlations according to

$$\left\langle s_j \dots s_k \dots s_l \right\rangle \approx \left\langle s_j \right\rangle \dots \langle s_k \rangle \dots \langle s_l \rangle. \tag{2.98}$$

Introducing the approximation (2.98) in Eqn. (2.96) with $\{f_i\} = 1.0$ we get

$$m = [\cosh(J\nabla) + m\sinh(J\nabla)]^z f(x)|_{x=0}. \tag{2.99}$$

Eqn. (2.99) can be written in a compact polynomial form by using the Binomial formula

$$m = \sum_{j=0}^{z} A_j m^j, \tag{2.100}$$

where the coefficients A_j are defined as

$$A_j = \begin{pmatrix} z \\ j \end{pmatrix} \cosh^{z-j}(J\nabla)\sinh^j(J\nabla) f(x)|_{x=0}, \tag{2.101}$$

which can be calculated numerically using the relation $e^{\alpha\nabla} f(x) = f(x+\alpha)$ where α is a constant variable. Following the same procedure and by using the exponential form of hyperbolic functions in Eqn. (2.101) we get

$$\cosh^{z-j}(J\nabla)\sinh^j(J\nabla) = \sum_{k=0}^{z-j}\sum_{s=0}^{j} \frac{(-1)^s}{2^z} \begin{pmatrix} z-j \\ j \end{pmatrix} \begin{pmatrix} j \\ s \end{pmatrix} \exp\left[(z-2k-2s)J\nabla\right]. \tag{2.102}$$

With the help of Eqs. (2.101) and (2.102), magnetization of the system can be easily evaluated as a function of temperature for any coordination number q from Eqn. (2.100). The total idea on decoupling the multi-spin correlations was proposed by

Zernike (Zernike, 1940). Similar description has been given by Yüksel (Yüksel, 2013).

2.5 Master Equation and Glauber Type-Stochastic Process

Let us consider a system that we can define all of the properties of a system with a single stochastic variable Y. Y may represents many different phenomenon such as the velocity of a Brownian particle, particle number in a box or the number of the people waiting in a line. We use the notation below for the probability density to characterize Y:

- $P_1(y_1,t_1)$ ≡(The probability density for y_1 value in time t_1 of the stochastic variable Y.)
- $P_2(y_1,t_1;y_2,t_2)$ ≡(The common probability density for y_1 value in time t_1 and y_2 value in time t_2 of the stochastic variable Y.)
- $P_n(y_1,t_1;y_2,t_2;\ldots;y_n,t_n)$ ≡ (The common probability density for y_1 value in time t_1, y_2 value in time t_2, …, y_n value in time t_n of the stochastic variable Y.)

Common probability densities is positive $P_n \geq 0$ in all time and one can reduces as,

$$\int P_n(y_1,t_1;y_2,t_2;\ldots;y_n,t_n) = P_{n-1}(y_1,t_1;y_2,t_2;\ldots;y_{n-1},t_{n-1}). \tag{2.103}$$

Common probability densities are normalized at the same time:

$$\int P_n(y_1,t_1)dy_1 = 1. \tag{2.104}$$

Here, the relevant stochastic variable Y is assumed as continuous. Otherwise, we have to replace the integrals in Eqn. (2.103) and (2.104) with summation. Thus, by defining the standard correlation between each stochastic variable in different times:

$$\langle y_1(t_1)y_2(t_2)\ldots y_n(t_n)\rangle = \int\int\ldots\int y_1y_2\ldots y_nP_n(y_1,t_1;y_2,t_2;\ldots;y_n,t_n)dy_1\ldots dy_n. \tag{2.105}$$

If the related process which is defined for all n and τ satisfies this condition,

$$P_n(y_1,t_1;y_2,t_2;\ldots;y_n,t_n) = P_n(y_1,t_1+\tau;y_2,t_2+\tau;\ldots;y_n,t_n+\tau), \tag{2.106}$$

then it is stable. Hence, for a stable process we can define

$$P_1(y_1,t_1) = P_1(y_1) \tag{2.107}$$

and the correlation $\langle y_1(t_1)y_2(t_2)\rangle$ only depends on the absolute difference between times $|t_1 - t_2|$. All the equilibrium process are stable. Here, we have to define a new conditional probability: $P_{1|1}(y_1,t_1|y_2,t_2) \equiv$ (conditional probability of being y_2 value in time t_2 for the stochastic variable Y has y_1 value in time t_1). And the related conditional probability can be defined as

$$P_1(y_1,t_1)P_{1|1}(y_1,t_1|y_2,t_2) = P_2(y_2,t_2) \tag{2.108}$$

then by using Eqn. (2.103) and (2.108), one can get the equation below for the probability density with different times

$$P_1(y_2,t_2) = \int P_1(y_1,t_1)P_{1|1}(y_1,t_1|y_2,t_2)dy_1. \tag{2.109}$$

In here the conditional probability density has the property

$$\int P_{1|1}(y_1,t_1|y_2,t_2)dy_2 = 1. \tag{2.110}$$

Now we can easily make a claim about the common conditional probability density:

- $P_{k|l}(y_1,t_1;\ldots;y_k,t_k|y_{k+1},t_{k+1};\ldots;y_{k+l},t_{k+l}) \equiv$ The common conditional probability density of being at the values $(y_{k+1},t_{k+1};\ldots;y_{k+l},t_{k+l})$ of the stochastic variable Y for given values $(y_1,t_1;\ldots;y_k,t_k)$.

So,

$$P_{k|l}(y_1,t_1;\ldots|\ldots;y_{k+l},t_{k+l}) = \frac{P_{k+1}(y_1,t_1;\ldots;y_k,t_k;y_{k+1},t_{k+1};\ldots;y_{k+l},t_{k+l})}{P_k(y_1,t_1;\ldots;y_k,t_k)} \quad (2.111)$$

When there is a correlation between the values of stochastic variables in different times, the common conditional probability densities become important. On the other hand, the stochastic variable only depends on it's intrinsic time then common conditional probability density and the common probability density have not important roles. In the first situation the common conditional probability density has the form

$$P_{n-1|1}(y_1,t_1;\ldots;y_{n-1},t_{n-1}|y_n,t_n) = P_{1|1}(y_{n-1},t_{n-1}). \quad (2.112)$$

Here, it occurs automatically an sequence like $t_1 < t_2 < \ldots < t_n$. That is to say, each steps determines from only the step coming before itself, namely, y_n conditional probability in time t_n determines from y_{n-1} conditional probability in time t_{n-1}. Is is not not affected by the earlier times step. The absence of any conditional probability is called *transition probability* as we as a standard process consistent with the condition in Eqn. (2.103) is called Markov chain. Let us define a Markov chain by using only the two functions as $P_1(y,t)$ and $P_{1|1}(y_1,t_1|y_2,t_2)$. The hierarchy of the probability density can be established from these functions. For example,

$$\begin{aligned} P_3(y_1,t_1;y_2,t_2;y_3,t_3) &= P_2(y_1,t_1;y_2,t_2)P_{2|1}(y_1,t_1;y_2,t_2;y_3,t_3) \\ &= P_1(y_1,t_1)P_{1|1}(y_1,t_1;y_2,t_2)P_{1|1}(y_1,t_1;y_3,t_3). \end{aligned} \quad (2.113)$$

By integrating Eqn. (2.113) over y_2 under $t_1 < t_2 < t_3$;

$$P_2(y_1,t_1|y_3,t_3) = P_1(y_1,t_1)\int P_{1|1}(y_1,t_1|y_2,t_2)P_{1|1}(y_2,t_2|y_3,t_3)dy_2, \quad (2.114)$$

and dividing both sides by $P_1(y_1,t_1)$ we get

$$P_{1|1}(y_1,t_1|y_3,t_3) = \int P_{1|1}(y_1,t_1|y_2,t_2)P_{1|1}(y_2,t_2|y_3,t_3)dy_2. \quad (2.115)$$

Eqn. (2.115) is called *Chapman-Kolmogorov* equation. We have to note that the transition probability from (y_1, t_1) to (y_3, t_3) has been separated as two steps; first from (y_1, t_1) to (y_2, t_2) and the second one from (y_2, t_2) to (y_3, t_3). These steps are statistically independent between each others. The defined transition such as $(y_2, t_2) \rightarrow (y_3, t_3)$ does not affect by the previous transition $(y_1, t_1) \rightarrow (y_2, t_2)$.

2.5.1 Markov Chains

Markov chains can be given as one of the most simple example of Markovian process (Reichl, 1997). These chains include the transitions of stochastic variable Y in discrete time intervals. Let us assume that Y is the realization of $\{y(n)\}$ where $n = 1, 2, \ldots, M$ and transitions occurs at the times $t = s\tau$ where $s = 0, 1, \ldots, \infty$. $P(n, s)$ represents having the $y(n)$ realization in time $t = s$. Also, $P_{1|1}(n_1, s_1|n_2, s_2)$ represents having the conditional probability the $y(n_2)$ realization in time s_2 in the absence of the $y(n_1)$ realization in time s_1 of Y. Markov chain is completely determined by using two functions $P(y, t)$ and $P_{1|1}(y_1, t_1|y_2, t_2)$. So the probability density hierarchy can be generated from these functions. Eqn. (2.113) can be written down for $P(n, s)$ as follows,

$$P(n, s+1) = \sum_{m=1}^{M} P(m, s) P_{1|1}(m, s|n, s+1). \tag{2.116}$$

The conditional probability can be formulized from Chapman-Kolmogorov equation,

$$P_{1|1}(n_0, s_0|n, s+1) = \sum_{m=1}^{M} P_{1|1}(n_0, s_0|m, s) P_{1|1}(m, s|n, s+1), \tag{2.117}$$

where $P_{1|1}(m, s|n, s+1)$ is the transition probability. Jumping to the n state in next step from the m state in time s is conditional probability.

2.5.2 Derivation of The Master Equation

Now, we must have a differential equation including time dependent probability. We consider the process depending on the time interval between each snapshot of the system is so closed. The time evolution of such systems is given by *master equation*.

Let us rewrite Eqn. (2.109);

$$P_1(n,t+\Delta t) = \sum_{m=1}^{M} P_1(m,t)P_{1|1}(m,t|n,t+\Delta t). \tag{2.118}$$

The related differential equation for $P_1(n,t)$ is as follows,

$$\frac{\partial P_1(n,t)}{\partial t} \equiv \lim_{\delta t\to 0}\left(\frac{P(n,t+\Delta)-P_1(n,t)}{\Delta t}\right), \tag{2.119}$$

$$\equiv \lim_{\Delta t\to 0}\frac{1}{\Delta t}P_1\Big((m,t)P_{1|1}(m,t|n,t+\Delta t)-\delta_{m,n}\Big). \tag{2.120}$$

We can also use the Taylor series expansion to handle $P_{1|1}(m,t|n,t+\Delta t)$. In order to keep conservative probability in each time step, we use the usual from as,

$$P_{1|1}(m,t|n,t+\Delta t) = \delta_{m,n}\left[1-\Delta t\sum_{l=1}^{M} w_{m,l}(t)\right] + w_{m,n}(t)\Delta t + \ldots, \tag{2.121}$$

where $w_{m,n}(t)$ is the transition probability and $w_{m,n}(t)\Delta t$ is the transition probability from the state m to n in $t \to t+\Delta t$. Similarly, the expression $[1-\Delta t\sum_{l=1}^{M} w_{m,l}(t)]$ corresponds to any absence of any transition in the time interval $t \to t+\Delta t$. When we insert Eqn. (2.121) in Eqn. (2.119) then we get,

$$\frac{\partial P_1(n,t)}{\partial t} = \sum_{m=1}^{M}\left[P_1(m,t)w_{m,n}(t) - P_1(n,t)w_{m,n}(t)\right]. \tag{2.122}$$

This equation is called *master equation*. Master equation gives the rate of the transitions from all other states to the state n and the to the rest of the states. Conditional probability ($P_{1|1}(n_0,0|n,t)$) satisfies a master equation.

$$\frac{\partial P_{1|1}(n_0,0|n,t)}{\partial t} = \sum_{m=1}^{M}\Big[P_{1|1}(n_0,0|m,t)w_{m,n}(t) - P_{1|1}(n_0,0|n,t)w_{n,m}(t)\Big], \tag{2.123}$$

where $P_{1|1}(n_0,0|n,t)$ is the probability of being in state n at time t of a system which is in the state n_0 at time $t=0$. Conditional probability also satisfies the initial-value condition $P_{1|1}(n_0,0|n,0) = \delta_{n,n_0}$. We can easily write down more compact form of the

master equation by using transition matrix,

$$W_{m,n}(t) = w_{m,n}(t) - \delta \sum_{n=1}^{M} w_{m,n'}(t). \tag{2.124}$$

Hence, the form of the master equation

$$\frac{\partial P_1(n,t)}{\partial t} = \sum_{m=1}^{M} P_1(n,t) W_{m,n}(m,n)(t). \tag{2.125}$$

The transition matrix in Eqn. (2.124) must satisfies the both condition $W_{m,n} \geq 0$ (for $n \neq m$) and $\sum_n W_{m,n} = 0$ (for each m). Also, we can write down again more compact (2.125) by using Dirac notation. Let, $P_1(n,t) = \langle p(t)|n\rangle$, and here $\langle p(t)|$ is the probability vector and the quantity $P(t_0|t)$ in the equation $P_{1|1}(n_0,t_0|n,t) = \langle n_0|P(t_0,t)|n\rangle$ is conditional probability operator. Similarly, $W_{m,n}(t) = \langle m|W(t)|n\rangle$. Thus, the new form of the master equation by considering the probability operators and conditional probability operators is

$$\frac{\partial \langle p(t)|}{\partial t} = \langle p(t)|W(t)\rangle, \tag{2.126}$$

$$\frac{\partial \langle P(0|t)|}{\partial t} = P(0|t)W(t). \tag{2.127}$$

2.5.3 Detailed Balance

Detailed balance can be ensured in the event of transition rate as

$$P^s(n) w_{n,m} = P^s(m) w_{m,n}, \tag{2.128}$$

where the expression $P^s \equiv \lim_{t\to\infty} P_l(n,t)$ is the long-life stability probability of the system (we assumed that the transition probabilities are not depend on time). $P^{s](n)}$ is the bra eigenvector of the transition matrix. Eqn. (2.128) tells us that the probability flow from m to n and from n to m are equal in equilibrium. We can get $P^s(n)$ by iterating Eqn. (2.128). For example, by sequencing $P^s(2) = P^s(1)(w_{1,2/w_{3,2}})$ ve $P^s(3) = P^s(2)(w_{2,3}/w_{3,2}) = P^s(1)(w_{1,2}/w_{2,1})(w_{2,3}/w_{3,2})$. The expression $P^s(1)$ can be found

from the normalization property. The dynamical evolution of the master equation given in Eqn. (2.128) can be easily shown by using a symmetrical matrix:

$$\begin{aligned} V_{n,m} &= \sqrt{\frac{P^s(n)}{P^s(m)}} W_{n,m} = \sqrt{\frac{P^s(n)}{P^s(m)}} w_{n,m} - \delta_{n,m} \sum_{n'} w_{n,n'} \\ &= \sqrt{\frac{P^s(n)}{P^s(m)}} w_{m,n} - \delta_{n,m} \sum_{n'} w_{m,n'} = V_{m,n'}. \end{aligned} \tag{2.129}$$

Let us define a new function in the form of $\tilde{P}(n,t) = P_1(n,t)/\sqrt{P^s(n)}$, hence the form of the master equation is as follows,

$$\frac{\partial \tilde{P}(n,t)}{\partial t} = \sum_{m=1}^{M} \tilde{P}(m,t) V_{m,n'}. \tag{2.130}$$

Here, we must again use the Dirac notation and write the equalities $\langle \tilde{p}(t)|n\rangle = \tilde{P}(n,t)$ and $V_{n,m} = \langle n|V|m\rangle$. The solution of the master equation,

$$\langle \tilde{p}(t)| = \langle \tilde{p}(0)|e^{Vt}. \tag{2.131}$$

$V_{n,m}$ is a symmetrical matrix and it has also a set of orthonormal eigenvector. The eigenvalues and eigenvectors of V can be shown as λ_i and $\langle \psi_i|$ and $|\psi_i\rangle$ respectively; where $i = 0, \ldots, M-1$. Bra and ket are similar.

2.5.4 Glauber Model for A Spin System

At first, we consider a single spin in contact with a heat bath. In this case, the spin interaction with the heat bath will causes to switch of the spin's state from one to another (spin-flip) in a certain transition. We have to use probability function $p(s,t)$ to exactly determine the overall behavior of the system. Probability function firstly satisfy the normalization condition,

$$\sum_{s_j=\pm 1} p(s_j,t) = p(1,t) + p(-1,t) = 1. \tag{2.132}$$

In order to calculate the probability function, the way that we have to follow is to write down the related differential equation and to obtain the function by solving that equation. The equation will includes two terms. The first one explain the probability of spin flip from the state to any others and it will correspond to the product of the transition probability per unit time and probability function. We must put a minus sign at the head of the first term because of the transition induced decreasing probability. The second one explain a transition from any other state to the present state. So, the sign of the second term will be plus just because of the contribution of the current situation of system.

$$\frac{d}{dt}p(s,t) = -\omega(s)p(s,t) + \omega(-s)p(-s,t). \tag{2.133}$$

Finally this equation is called *master equation*. There exists 2^N equation for the system with N particle. As one would expect that is not possible to solve the master equation exactly except a few very simple system. However, it is possible for a simple system consisting of a single spin. For this purpose, it would be appropriate to introduce a function such as

$$\begin{aligned} Q(t) &= \sum_{s_j=\pm 1} s_j p(s_j,t) \\ &= p(1,t) - p(-1,t). \end{aligned} \tag{2.134}$$

With the help of normalization condition, $p(s,t)$ is in the form of

$$p(s,t) = \frac{1}{2}(1 + sQ(t)). \tag{2.135}$$

Besides, from the definition of $Q(t)$ we can find out the probability function for the system consists one spin as follows,

$$p(\pm 1,t) = \frac{1}{2}(1 \pm sQ(t)). \tag{2.136}$$

After some algebraic continuation, we can construct the dynamical equation of state which is based on the time evaluation of $Q(t)$:

$$\frac{d}{dt}Q(t) = -2\omega Q(t). \tag{2.137}$$

Thus the solution of Eqn. (2.137),

$$Q(t) = Q(0)\exp(-2\omega t). \tag{2.138}$$

Here, $Q(t)$ is an exponentially decreasing function and it goes to zero in equilibrium. This corresponds to the zero magnetization in equilibrium and completely consistent with equilibrium case.

2.5.5 Glauber Model For N-Spin System

In this subsection, we build the equation of state for a ferromagnetic kinetic Ising-type system which consists N spins. The master equation for N spins is in the form of

$$\begin{aligned}\frac{d}{dt}P(S_1,\ldots,S_N;t) = &- \sum_i \sum_{S_i \neq S_{i'}} \omega_i(S_i \to S_{i'})P(S_i,\ldots,S_i,\ldots,S_N;t) \\ &+ \sum_i \sum_{S_i \neq S_{i'}} \omega_i(S_{i'} \to S_i)P(S_1,\ldots,S_{i'},\ldots,S_N;t),\end{aligned} \tag{2.139}$$

where $P(S_1,\ldots,S_N;t)$ is the probability of the $(S_1,\ldots,S_N;t)$ configuration in time t. The first term in the right-hand side of Eqn. (2.139) stands for decreasing of probability (flip out) and the second term represents the increasing of such probability by a transition from any other state to present state. On the other hand, the distribution getting from by the solution of the master equation must be compatible with the canonical distribution in equilibrium. The energy of the system for the kinetic spin-1/2 Ising model is given as

$$\mathcal{H} = -\frac{J}{N}\sum_{\langle ij\rangle} S_i S_j - H(t)\sum_i S_i. \tag{2.140}$$

Here, J, S_i and $H(t)$ are exchange interaction, spin variable and oscillatory external magnetic field respectively. $S = \pm 1/2$ and $J > 0$ for spin-1/2 system. Additionally, external field clearly in the form of

$$H(t) = H_0 \cos(\omega t). \tag{2.141}$$

The system evaluates with time scale τ. τ is the switching time for a single spin. The transition probability corresponds the spin-flip of ith spin in time t and it is shown as ω_i. Hence, the transition probability within the Glauber-type stochastic process is

$$\omega_i = \frac{1}{2\tau}(1 - S_i \tanh(\beta E_i)). \tag{2.142}$$

Here, E_i is the effective-field and it is in the form of

$$E_i = \frac{J}{N} \sum_{j \neq i} S_j + H(t). \tag{2.143}$$

After all, dynamical equation of state which describes the time evaluation of the average spin moment is as follows

$$\tau \frac{d}{dt} \langle S_i \rangle = -\langle S_i \rangle + \tanh(\beta E_i). \tag{2.144}$$

The final form of the Eqn. (2.144) is

$$\Omega \frac{dm}{d\xi} = -m + \tanh\left(\frac{1}{T}(m + h\cos\xi)\right), \tag{2.145}$$

where $m = \langle S_i \rangle$ and $\xi = \omega t$. Additionally, $T = (\beta J)^{-1}$, $h = H_0/J$ and $\Omega = \omega\tau$ are the dimensionless quantities.

By solving Eqn. (2.145) we can get the sinusoidally oscillating magnetization, namely magnetization time series, and then if we integrate over a time period of it then occurs the DOP.

For more details, see (Vatansever, 2011).

CHAPTER THREE
METHODOLOGY

In this chapter, we will give the application of EFT formalism to dynamical Ising-type thin films.

3.1 Construction of The Self-Consistent Dynamical Equations of States

From the theoretical point of view, the most widely used model to study the magnetic properties of surfaces is the Ising model due to the crossover of dimensionality and strong uniaxial anisotropy. Hence, in order to investigate the dynamical transitions, surface enhancement phenomenon, dynamical symmetry breaking, strength of the magnetic order in different layers and many other dynamical features, we choose dynamical Ising-typed simple cubic isometry which has an inner coordination number $z = 4$ defined in three dimension with a time dependent external oscillatory (in time but uniform over the space) magnetic field studied by EFT. For this purpose, we consider the following Hamiltonian,

$$\mathcal{H} = -\sum_{\langle ij \rangle} J_{ij} s_i s_j - h(t) \sum_i s_i \tag{3.1}$$

where s_i is the spin operator on lattice site i and any spin variable can take the values $s_i = \pm 1$. $\langle \ldots \rangle$ subscript bracket symbolizes the nearest neighboring in the first summation. The second summation is over all the lattice sites. The exchange interaction J_{ij} between the spins on the sites i and j take the values according to the positions of the nearest neighbor spins. Two surfaces of the film have intralayer coupling J_1. The interlayer coupling between the surface and its adjacent layer (i.e. layers 1, 2 and L, $L-1$) is denoted by J_2. For the rest of the layers, the interlayer and the intralayer couplings are assumed as J_3. The system has three exchange interactions where J_1, J_2, $J_3 > 0$ favors a ferromagnetic alignment of the adjacent sites as shown in Fig. 3.1. The Zeeman term describes interaction of the spins with the field of the sinusoidal form

$$h(t) = h_0 \cos(\omega t), \tag{3.2}$$

where t is the time and h_0 is the amplitude of the oscillatory magnetic field with an angular frequency ω.

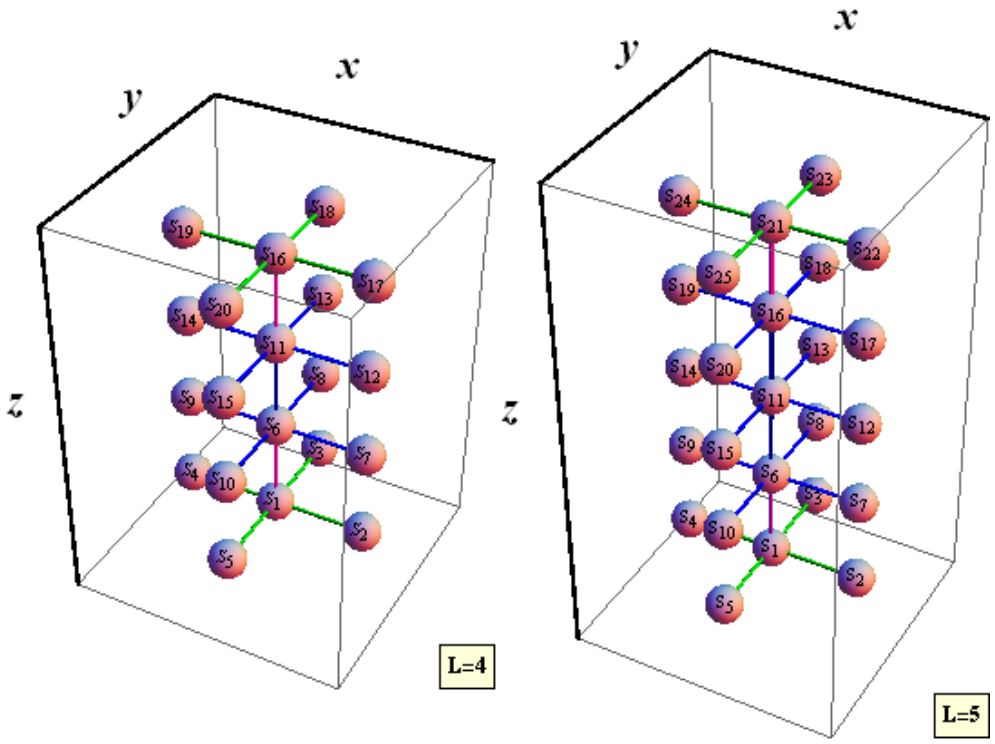

Figure 3.1 Magnetic unit cell for the simple cubic thin films of two different thicknesses as $L = 4, 5$. The lattice has a finite size only in z direction as other two directions are defined on the interval such that $x, y \epsilon (-\infty, \infty)$. Green, magenta and blue cylindrical edges represent J_1, J_2, J_3 ferromagnetic exchanges respectively, as well as spherical vertices symbolize the magnetic items.

Conventionally, the layer agents remaining invariant under the appropriate symmetry operation in a bulk system are defined with certain criterions: Spin values, types and number of its neighboring interactions. The relevant agents depict thermo-magnetical behavior of whole material whereas in more realistic systems (such as magnetic thin films), one should construct the equations of state for each layer agents to control the dependency of the characteristics with the film thickness hence, such criterion-related validity is lost. Our system is in contact with an isothermal heat bath at given temperature T. So, the dynamical evolution of the system may be given by non-equilibrium Glauber dynamics (Glauber, 1963) based on a master equation. The

dynamical equations of motion for each layer are in the form of

$$\tau\frac{d}{dt}\langle s_i^{(k)}\rangle = -\langle s_i^{(k)}\rangle + \langle \tanh[\beta(E_i^{(k)} + h(t))]\rangle, \quad k = 1, \ldots, L \tag{3.3}$$

with

$$\begin{aligned}
E_i^{(1)} &= \sum_{\delta=1}^{z} J_1 s_\delta^{(1)} + J_2 s_{\delta'}^{(2)}, \\
E_i^{(2)} &= J_2 s_{\delta'}^{(1)} + \sum_{\delta=1}^{z} J_3 s_\delta^{(2)} + J_3 s_{\delta'}^{(3)}, \\
&\vdots \quad \vdots \qquad\qquad \vdots \\
E_i^{(k)} &= J_3 s_{\delta'}^{(k-1)} + \sum_{\delta=1}^{z} J_3 s_\delta^{(k)} + J_3 s_{\delta'}^{(k+1)}, \\
&\vdots \quad \vdots \qquad\qquad \vdots \\
E_i^{(L-1)} &= J_3 s_{\delta'}^{(L-2)} + \sum_{\delta=1}^{z} J_3 s_\delta^{(L-1)} + J_3 s_{\delta'}^{(L)}, \\
E_i^{(L)} &= J_2 s_{\delta'}^{(L-1)} + \sum_{\delta=1}^{z} J_1 s_\delta^{(L)},
\end{aligned} \tag{3.4}$$

where $1/\tau$ is the transition per unit time in a Glauber type stochastic process, $\beta = 1/k_B T$ and k_B represents the Boltzmann constant. The subscript and superscript in a spin variable symbolizes the lattice site and layer number respectively as well as $E_i^{(k)}$ is the local field acting on the site i in kth layer. δ and δ' subscripts in the energy contributions represent in-layer and out-of-layer nearest neighboring and this type of indication also is reinforced by superscripting with regard to control the relation between production index and the nearest neighboring argument in progressive aspects. The average brackets in Eqn. (3.3) stand for the usual canonical thermal average.

In order to handle the second term on the right-hand side of the Eqn. (3.3) we use the differential operator technique (Honmura & Kaneyoshi, 1979). By using the technique, Eqn. (3.3) gets in the form of

$$\tau\frac{d}{dt}\langle s_i^{(k)}\rangle = -\langle s_i^{(k)}\rangle + \langle \exp(E_i^{(k)}\nabla)\rangle f(x)|_{x=0}, \quad k = 1, \ldots, L \tag{3.5}$$

where $\nabla = \partial/\partial x$ is one dimensional differential operator and the function $f(x)$ is given by

$$f(x) = \tanh[\beta(x + h(t))], \tag{3.6}$$

as for that the effect of the differential operator on a function $f(x)$,

$$\exp(a\nabla) f(x)|_{x=0} = f(x + a)|_{x=0}, \tag{3.7}$$

with any real constant a. By using the energy expression given in Eqn. (3.4), in Eqn. (3.5) then, in order to get a polynomial form of the second term on the right-hand side of the equations, by using the van der Waerden identity for two-state spin, i.e., $\exp(bs_i) = \cosh(b) + s_i \sinh(b)$ where b is any real constant in a representative manner, we write the exponential term in terms of the hyperbolic trigonometric functions then Eqn. (3.5) exactly written in terms of multiple spin correlation functions occurring on the right-hand side. Thus we get

$$\begin{aligned}
\tau\frac{d}{dt}\langle s_i^{(1)}\rangle &= -\langle s_i^{(1)}\rangle + \left\langle \prod_{\delta=1}^{z} [A_1 + s_\delta^{(1)} B_1][A_2 + s_{\delta'}^{(2)} B_2] \right\rangle, \\
\tau\frac{d}{dt}\langle s_i^{(2)}\rangle &= -\langle s_i^{(2)}\rangle + \left\langle [A_2 + s_{\delta'}^{(1)} B_2] \prod_{\delta=1}^{z} [A_3 + s_\delta^{(2)} B_3][A_3 + s_{\delta'}^{(3)} B_3] \right\rangle, \\
\vdots \quad & \quad \vdots \qquad\qquad\qquad\qquad \vdots \\
\tau\frac{d}{dt}\langle s_i^{(k)}\rangle &= -\langle s_i^{(k)}\rangle + \left\langle [A_3 + s_{\delta'}^{(k-1)} B_3] \prod_{\delta=1}^{z} [A_3 + s_\delta^{(k)} B_3][A_3 + s_{\delta'}^{(k+1)} B_3] \right\rangle, \\
\vdots \quad & \quad \vdots \qquad\qquad\qquad\qquad \vdots \\
\tau\frac{d}{dt}\langle s_i^{(L-1)}\rangle &= -\langle s_i^{(L-1)}\rangle + \left\langle [A_3 + s_{\delta'}^{(L-2)} B_3] \prod_{\delta=1}^{z} [A_3 + s_\delta^{(L-1)} B_3][A_2 + s_{\delta'}^{(L)} B_2] \right\rangle, \\
\tau\frac{d}{dt}\langle s_i^{(L)}\rangle &= -\langle s_i^{(L)}\rangle + \left\langle [A_2 + s_{\delta'}^{(L-1)} B_2] \prod_{\delta=1}^{z} [A_1 + s_\delta^{(L)} B_1] \right\rangle,
\end{aligned} \tag{3.8}$$

with

$$\begin{aligned}
A_n &= \cosh(J_n \nabla) f(x)|_{x=0}, \\
B_n &= \sinh(J_n \nabla) f(x)|_{x=0},
\end{aligned} \tag{3.9}$$

where $n = 1, 2, 3$.

When the product in Eqn. (3.8) is expanded, the multi site spin correlations appear. In order to make the expansion manageable let us handle these correlations with a decoupling approximation (DA) (Tucker, 1991) as

$$\langle s_i^{(k)} \dots s_j^{(k)} \dots s_l^{(k)} \rangle = \langle s_1^{(k)} \rangle \dots \langle s_j^{(k)} \rangle \dots \langle s_l^{(k)} \rangle. \tag{3.10}$$

In fact, the primitive form of this improvement corresponds essentially to the Zernike approximation (Zernike, 1940) in the bulk problem and there exists an utilization of it on several magnetic systems including the surface problems (Balcerzak, 1991; Kaneyoshi et al., 1984, 1983). By using the expansion in Eqn. (3.10) and the assumption below

$$\langle s_i^{(k)} \rangle = m_k, \quad k = 1, \dots, L, \tag{3.11}$$

the Eqn. (3.8) morph into the form of,

$$\begin{aligned}
\tau \frac{dm_1}{dt} &= -m_1 + [A_1 + m_1 B_1]^z [A_2 + m_2 B_2], \\
\tau \frac{dm_2}{dt} &= -m_2 + [A_2 + m_1 B_2][A_3 + m_2 B_3]^z [A_3 + m_3 B_3], \\
\vdots \quad &\vdots \qquad\qquad\qquad \vdots \\
\tau \frac{dm_k}{dt} &= -m_k + [A_3 + m_{k-1} B_3][A_3 + m_k B_3]^z [A_3 + m_{k+1} B_3], \\
\vdots \quad &\vdots \qquad\qquad\qquad \vdots \\
\tau \frac{dm_{L-1}}{dt} &= -m_{L-1} + [A_3 + m_{L-2} B_3][A_3 + m_{L-1} B_3]^z [A_2 + m_L B_2], \\
\tau \frac{dm_L}{dt} &= -m_L + [A_2 + m_{L-1} B_2][A_1 + m_L B_1]^z.
\end{aligned} \tag{3.12}$$

By using the binomial expansion and writing the hyperbolic trigonometric functions in

terms of the exponential functions we get the most compact form of Eqn. (3.12) as

$$\begin{aligned}
\dot{m}_1 &= \frac{1}{\tau}\left(-m_1 + \sum_{\gamma=0}^{z}\sum_{\eta=0}^{1}\Lambda_1(\gamma,\eta)m_1^{\gamma}m_2^{\eta}\right),\\
\dot{m}_2 &= \frac{1}{\tau}\left(-m_2 + \sum_{\gamma=0}^{z}\sum_{\eta=0}^{1}\sum_{\nu=0}^{1}\Lambda_2(\gamma,\eta,\nu)m_2^{\gamma}m_1^{\eta}m_3^{\nu}\right),\\
\vdots \quad &\vdots \qquad\qquad\qquad \vdots\\
\dot{m}_k &= \frac{1}{\tau}\left(-m_k + \sum_{\gamma=0}^{z}\sum_{\eta=0}^{1}\sum_{\nu=0}^{1}\Lambda_3(\gamma,\eta,\nu)m_k^{\gamma}m_{k-1}^{\eta}m_{k+1}^{\nu}\right),\\
\vdots \quad &\vdots \qquad\qquad\qquad \vdots\\
\dot{m}_{L-1} &= \frac{1}{\tau}\left(-m_{L-1} + \sum_{\gamma=0}^{z}\sum_{\eta=0}^{1}\sum_{\nu=0}^{1}\Lambda_2(\gamma,\eta,\nu)m_L^{\gamma}m_{L-1}^{\eta}m_{L+1}^{\nu}\right),\\
\dot{m}_L &= \frac{1}{\tau}\left(-m_L + \sum_{\gamma=0}^{z}\sum_{\eta=0}^{1}\Lambda_1(\gamma,\eta)m_L^{\gamma}m_{L-1}^{\eta}\right).
\end{aligned} \tag{3.13}$$

where

$$\begin{aligned}
\Lambda_1(\gamma,\eta) &= \binom{z}{\gamma}\binom{1}{\eta}A_1^{z-\gamma}A_2^{1-\eta}B_1^{\gamma}B_2^{\eta},\\
\Lambda_2(\gamma,\eta,\nu) &= \binom{z}{\gamma}\binom{1}{\eta}\binom{1}{\nu}A_2^{1-\eta}A_3^{z+1-\gamma-\nu}B_2^{\eta}B_3^{\gamma+\nu},\\
\Lambda_3(\gamma,\eta,\nu) &= \binom{z}{\gamma}\binom{1}{\eta}\binom{1}{\nu}A_3^{z+2-\gamma-\eta-\nu}B_3^{\gamma+\eta+\nu}.
\end{aligned} \tag{3.14}$$

Note that, throughout our calculations $\tau = 1$ for simplicity. Self-consistent equations in Eqn. (3.13) are typical first order ordinary differential equations but have not an analytical solution because of the right-hand side contains transcendental functions. The dynamical equation of motion can be solved by various numerical methods. In this work, we prefer to use the fourth order Runge-Kutta method (RK4) to get the evolution of the $m(t)$ by regarding Eqn. (3.13) as an initial value problem. We can mention that the differential equation derived in Eqn. (3.13) extends up to the term m^z. Each term in the equation of motion makes contribution to the solution, because the value of m, which is calculated at each time step, is iteratively related to the previous m value, however the situation is different from the behavior of the equilibrium systems at which high ordered terms can be neglected in the neighborhood of phase transition

point.

3.2 Definitions and Declaration of Numerical Accuracy

The system has three dependent Hamiltonian variables, namely frequency of external magnetic field ω, amplitude h_0 and the film thickness L. For certain values of these parameters, temperature and the J_1, J_2, J_3 interaction constants, RK4 will give convergency behavior after some iterations i.e. the solutions have property $m(t) = m(t + 2\pi/\omega)$ for arbitrary initial value for the magnetization ($m(t = 0)$). Each iteration, i.e. the calculation of magnetization for $t+1$ from the previous magnetization for t, is now performed for these purpose whereby the RK4 iterative equation is being utilized to determine the magnetization for every i. In order to keep the iteration procedure stable in our simulations, we have chosen 10^4 points for each RK4 step. Thus, after obtaining the convergent region and some transient steps (which depends on Hamiltonian parameters and the temperature) the layer's average magnetization can be calculated from

$$Q_k = \frac{\omega}{2\pi} \oint m_k(t) dt \tag{3.15}$$

where m_k is a stable and periodic function anymore and finally the DOP can be calculated by the arithmetic mean as

$$Q = \frac{1}{L} \sum_{k=1}^{L} Q_k. \tag{3.16}$$

As cut-off condition for numerical self-consistency, we defined a tolerance

$$\left| Q_k|_{t-2\pi/\omega}^{t} - Q_k|_{t}^{t+2\pi/\omega} \right| < 10^{-5}, \tag{3.17}$$

meaning that the maximum error as difference between the each consecutive iteration should be lower than 10^{-5} for all steps. DOP accurately can be calculated from this stationary solutions of $m_k(t)$ over a cycle. On the other hand, the energy loss due to the hysteresis, in other words, HLA is defined as

$$A^{(k)} = -\oint m_k(t) dh(t) = h_0 \omega \oint m_k(t) \sin(\omega t), \tag{3.18}$$

and the modified surface exchange interaction has been defined to determine the different characteristic behavior of the system in certain range as

$$J_1 = J_3(1 + \Delta_s). \tag{3.19}$$

There are three possible order of the system: F, P and the coexistence phase (F+P). In P phase, $m(t)$ in convergent region for any layer is satisfied by this condition

$$m(t) = -m(t + \pi/\omega) \tag{3.20}$$

which is called the symmetric solution. On the other hand, in F phase, the solution does not satisfy Eqn. (3.20) and this solution is called as non-symmetric solution which oscillates around a non-zero magnetization value, and does not follow the external magnetic field i.e. the value of Q is different from zero. In these two cases, the observed behavior of magnetization is regardless of the choice of initial value of magnetization $m(0)$ whereas the last phase has magnetization solutions symmetric or non-symmetric depending on the choice of the initial value of magnetization corresponding to the coexistence region where F and P phases overlap. The main goal of our detailed investigation is adjunctly manifesting the frequency dispersion of the critical temperature coordinates of special point which can be calculated by benefiting from the phase diagrams in $(k_B T/J_3 - \Delta_s)$ planes for different field amplitudes in order to understand and clarify the behavior of the dynamical system, then to propound the frequency dispersion of HLA and corresponding coercivity ($H_c^{(k)}$) with remanence ($M_r^{(k)}$) of the layers.

CHAPTER FOUR
RESULTS PART-1: GLOBAL PHASE DIAGRAMS

The most appropriate values and/or intervals of parameters were chosen in our calculations to explain the whole dynamics with least-effort. Surface exchange J_1 was directly mapped onto Δ_s by-passing the distinction between bulk and interface exchange couplings as $J_2 \equiv J_3 = 1.0$. Unlike the deductive analysis, presenting the inferences as a result of investigation by induction is an essential principle in terms of understanding the overall behavior for such a scrutiny.

In this sense, variation of DOP with temperature for the selected different film thicknesses $L = 4, 7$ which was rigorously depicted in the text, constitutes as the starting point for our systematic investigation. The results were presented in Fig. 4.1 for two selected values of external field amplitude and for the major three frequency agents $h_0/J_3 = 1.0, 2.5$ and $\omega = 0.5, 1.0, 4.0$ respectively. The value of the crossover point Δ_s^* was calculated in accordance with the value reported by Kaneyoshi (Kaneyoshi, 1991). Slightly to the left and to the right of this point at $\Delta_s = 0.0053, 0.6053$ respectively, corresponding average layer magnetizations have contra-arranged strength of the magnetic order mutually. Thus, three representative values of the modified exchange also were taken and denoted from (a) to (b) as competence parameters $\Delta_s = 0.0053, 0.3053, 0.6053$. We also pointed out that this labeling procedure can be used for usual relevant behaviors in the same investigation from a different viewpoint, i.e. it was used for temperature dependency of the average magnetization of each layer in Fig. 4.2 and the variation of it with the layer index k at a fixed temperature where $k_BT/J_3 = 3.5$ in Fig. 4.3. Average magnetization profiles across the film differ qualitatively in two regimes ($\Delta_s < \Delta_s^*$ and $\Delta_s > \Delta_s^*$) as shown in Fig. 4.3 for the amplitude agents. The variation of DOP with temperature and consequently the critical temperature is independent from layer index and thickness L in the crossover point and this makes it 'special'. The thickness-independent critical temperature of the film at special point reduces to the bulk with coordination number $z = 6$ critical value $k_BT/J_3 = 5.0734$ in infinite-frequency for particular amplitude value

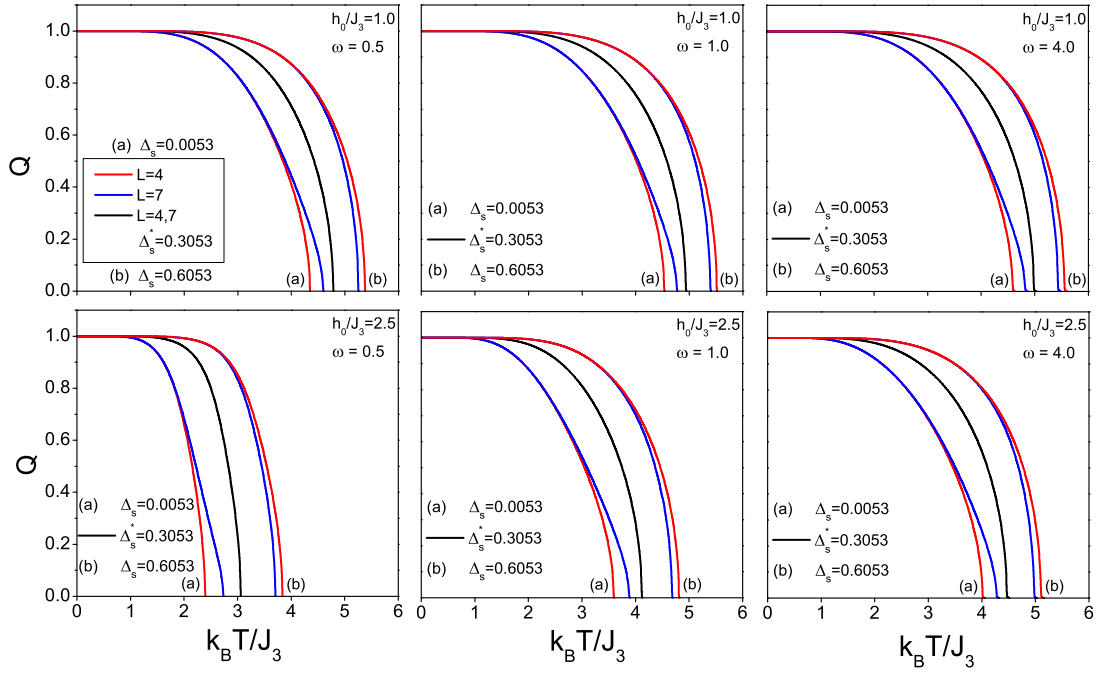

Figure 4.1 Variation of DOP with temperature for the selected films with different layers $L = 4, 7$. The calculations were performed for two values of external field amplitude. The left-hand- and right-hand-triple-panels correspond to $h_0/J_3 = 1.0, 2.5$ respectively an they can be seen for the major three frequency agents as $\omega = 0.5, 1.0, 4.0$. The number accompanying each set of curves denote the values of modified exchange from (a) to (b) as $\Delta_s = 0.0053, 0.3053, 0.6053$.

or zero-amplitude limit while there is no significant change in the value of the Δ_s^* when w or h_0 chances. This reduction is one of the major indicators for the accuracy of our treatment. The effect of external oscillatory magnetic field parameters on critical behavior of the bulk systems is now well known. At first sight, we can see in Fig. 4.1, 4.2, and 4.3 that a small increment in ω causes an increment in $k_B T_c/J_3$. However, an increment in h_0/J_3 causes a decreament $k_B T_c/J_3$ for given Δ_s and arbitrary ω. This is an expected result, since the increment in frequencies enhances the phase lag between time dependent magnetization and the external field signal. Therefore, the asymmetric behavior of hysteresis loop (HL) in the form of Lissajous curve, becomes more prominent, since the time dependent magnetization has less time to follow the oscillatory field. So, the system can undergo a DPT which requires a small amount of thermal energy. On the other hand, according to times-series of the magnetization and the external magnetic field, increasing the field frequency at first, obstructs the saturation of the ordinary magnetization due to the decreasing energy coming from the

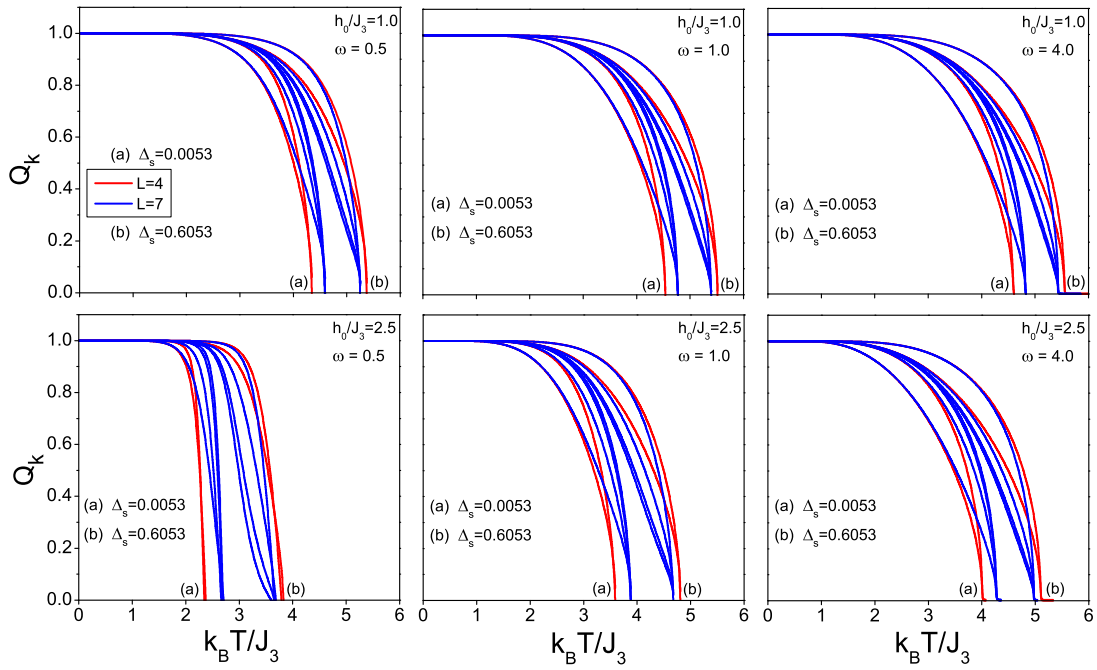

Figure 4.2 Variation of DOP for each layers with temperature for the selected films with different $L = 4, 7$ layers for two values of external field amplitude. The interchange of the layer hierarchy can be monitored in the figure for the same values depicted in Fig. 4.1.

oscillating magnetic field in a half-time period which facilitates the late stage domain growth by tending to align the moments in its direction (i.e. the magnetization begins to fail following the oscillatory field) and this makes the occurrence of the frequency increasing route to DPT at the critical point. There is a concurrence by different researchers that the HL loses its symmetry when the oscillating period of external perturbation becomes much smaller than the typical relaxation time of the system.

As stated in various place, a prime objective of the study was to confirm whether a common value of Δ_s exists for all films, and if so to determine its value. This requires a very accurate determination of the transition temperature for each film thickness and each value of surface exchange enhancement. For this purpose, we need to dart a glance at the relevant $(\Delta_s - k_B T/J_3)$ global phase diagrams are shown in Fig. 4.5. Those were plotted different numbers of layers when the strength of the field amplitude is $h_0/J_3 = 1.0, 2.5$ respectively. As Δ_s rises, the critical temperature of the system increases for arbitrary L. For each value of the frequency with the representative amplitudes, as seen clearly that the curves with different film thicknesses

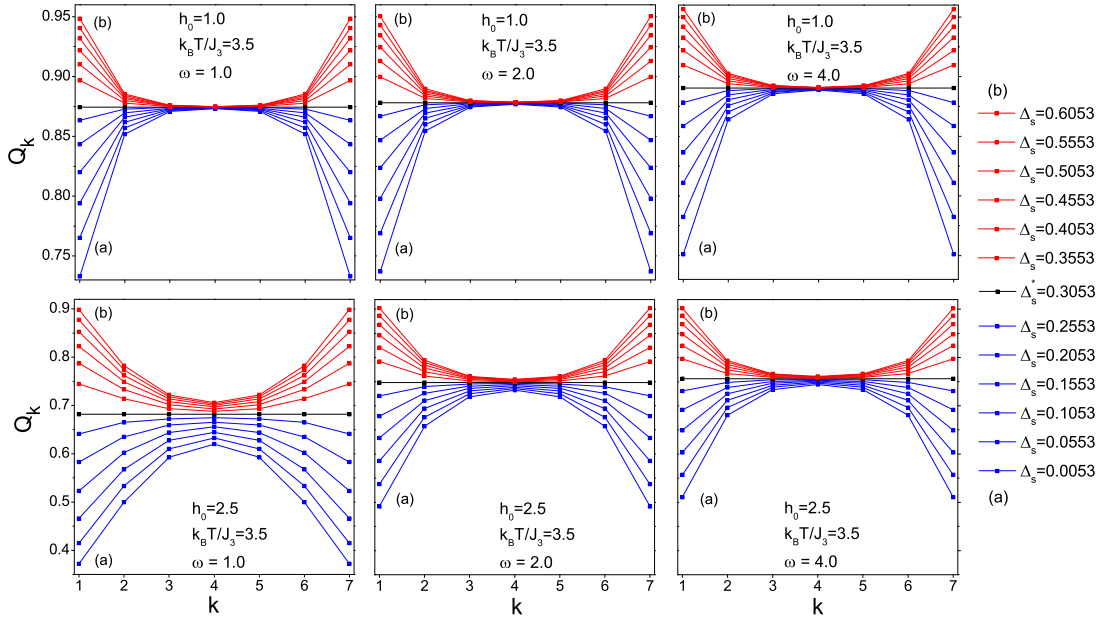

Figure 4.3 The average magnetization profiles for a film $L = 7$ layers for two values of external field amplitude $h_0/J_3 = 1.0, 2.5$ and fixed temperature $k_BT/J_3 = 3.5$. The number accompanying each curve denotes several values of modified exchange from (a) $\Delta_s = 0.0053$ to (b) $\Delta_s = 0.6053$. The evolution of the curves can be seen in the left-hand- and right-hand-triple-panels for the values of frequency $\omega = 0.5, 1.0, 4.0$.

intersect each other at the same abscissa point $\Delta_s = \Delta_s^* = 0.3053$. According to this result, the special point can be defined as that particular Δ_s value at which bulk critical temperature is independent of the film thickness L occurs. It is assumed to coincide with the critical temperature $k_BT_c^B/J_3$ of the corresponding isometric lattice (usual simple cubic lattice for the system under consideration). Furthermore, based on the definition of Δ_s, it can be expected that the crossover point in Fig. 4.5 should define also the critical temperature of three-dimensional infinite bulk system, where the surface and the Δ_s parameter are of no importance. This is really the case, which can be seen also from Fig. 4.5, where the bulk $k_BT_c^B/J_3$ and the surface $k_BT_c^S/J_3$ critical temperatures of the corresponding semi-infinite system are represented respectively by the dashed lines and also pointed by each arrow. For the values of $\Delta_s < \Delta_s^*$, thin films have lower critical temperature than the bulk system. The value of Δ_s also changes the relation between the thickness and the critical temperature of the film. k_BT_c/J_3 increases with the film thickness L, and approaches $k_BT_c^B/J_3$ asymptotically as the number of layers become large. The thicker films have higher critical values

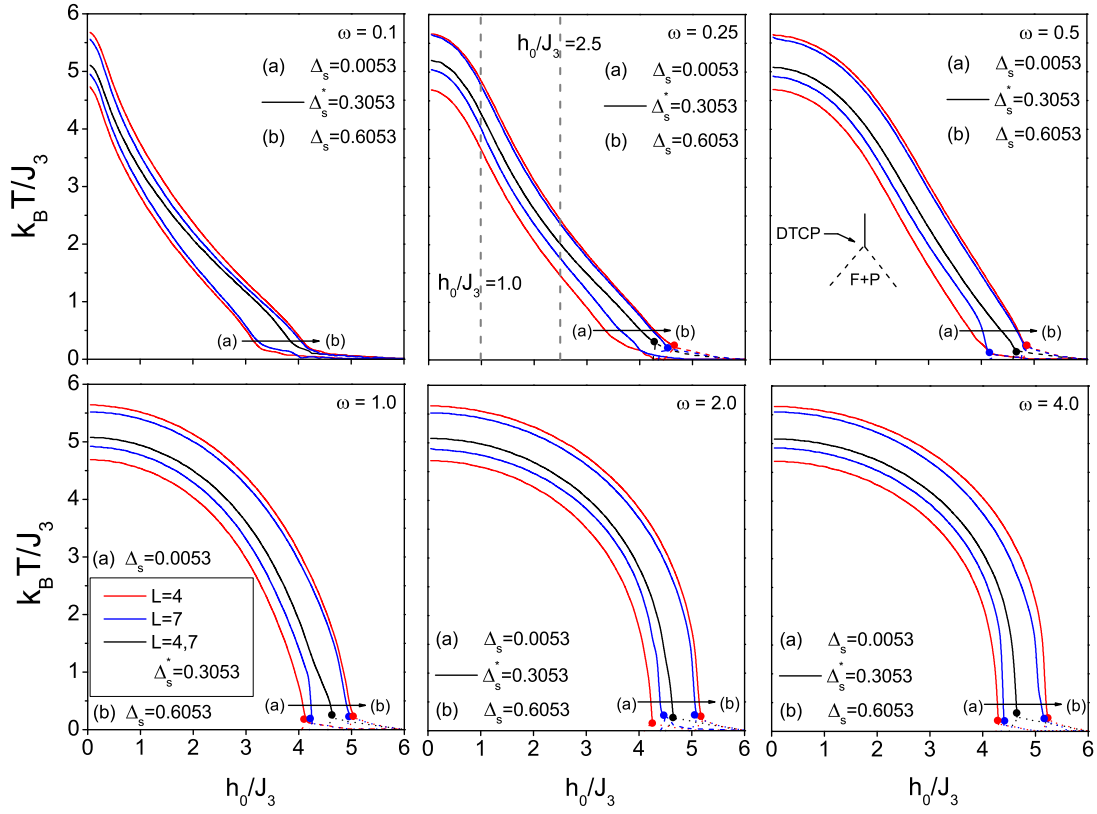

Figure 4.4 The phase diagram in the $(h_0/J_3 - k_BT/J_3)$ plane for the films with different $L = 4, 7$ layers. Frequency changes with $\omega = 0.1, 0.25, 0.5, 1.0, 2.0, 4.0$ for each panels. The numbers accompanying each set of curves denote the value of modified exchange from (a) to (b) as $\Delta_s = 0.0053, 0.3053, 0.6053$ and this displaying is also can be monitored in arrow's direction. The dashed lines in the middle-left-hand panel corresponding to the representatives serve as a viewing guide.

for $\Delta_s < \Delta_s^*$ whereas they have lower critical values for $\Delta_s > \Delta_s^*$ than thinner ones. It is worth noting once again that the critical temperature of the film is independent of L when $\Delta_s = \Delta_s^*$, and equal to $k_BT_c^B/J_3$. On the other hand, for $\Delta_s > \Delta_s^*$ the critical temperature k_BT_c/J_3 is greater than both the bulk $k_BT_c^B/J_3$ and the surface $k_BT_c^S/J_3$ critical temperatures of the corresponding semi-infinite Ising system and larger the L is, the lower k_BT_c/J_3 is. The film critical temperature k_BT_c/J_3 approaches asymptotically the surface critical temperature $k_BT_c^S/J_3$ of the corresponding semi-infinite system as the number of layers become large. Evolution of the curves with respect to frequency as $\omega = 0.1, 0.25, 0.5, 1.0, 2.0, 4.0$ for particular two amplitude agents as stated several times above $h_0/J_3 = 1.0, 2.5$ can be observed in Fig. 4.5. Accordingly, causes all the curves go-up (-down) with rising frequency (amplitude) value respectively also the same operation increases (decreases) the critical temperature of the system while it does no

affect the relation between the film thickness and critical temperature, i.e. for $\Delta_s < \Delta_s^*$ thicker films have higher critical values and reverse is valid for $\Delta_s > \Delta_s^*$ with $\omega, h_0 \neq 0$, if the special point present. In addition, there is no significant change in the abscissa point of the crossover (Δ_s^*) while rising or lowering of two oscillatory parameter transports the phase diagrams collectively in the space. When ω is large enough for finite amplitude value as $h_0 \neq 0$, the ordinate value of the special point approaches the bulk critical temperature in quasistatic case $k_B T_c^B / J_3$ asymptotically. The observations about dynamical feature of the global phase diagrams in $(\Delta_s - k_B T/J_3)$ planes can also be explained by the well known mechanism underlying the DPT phenomena. In other words, the aforementioned scenario is onset as things stand.

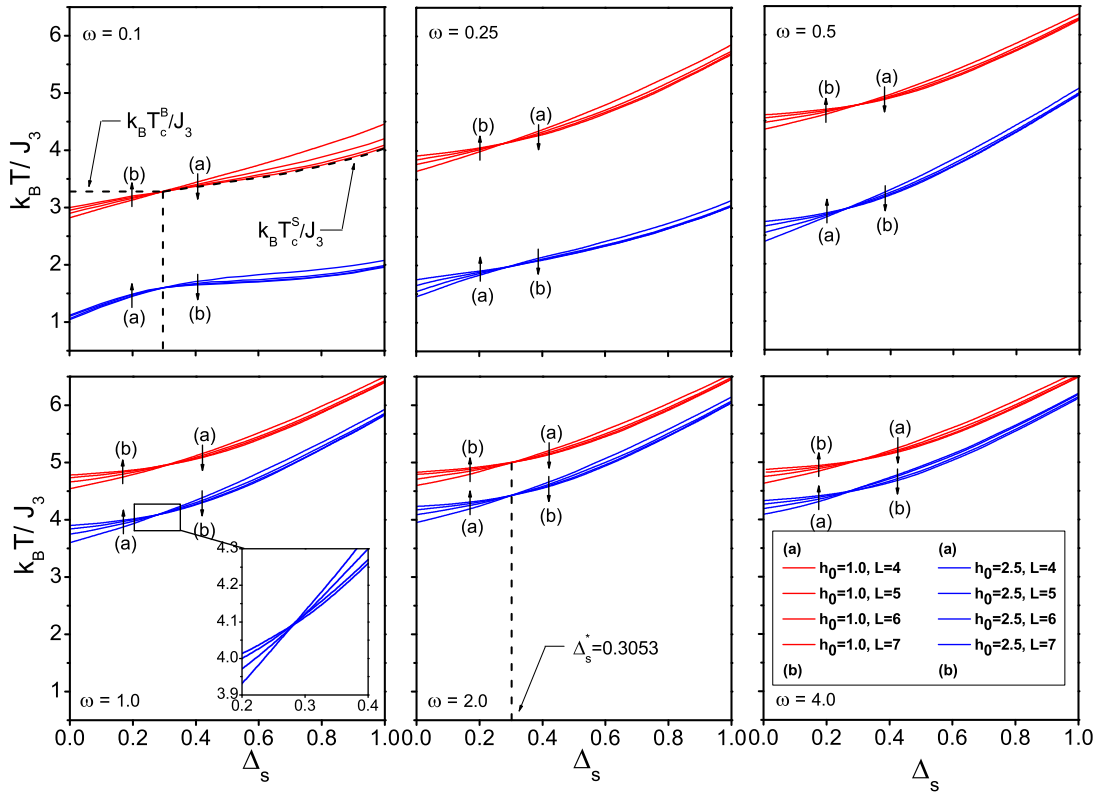

Figure 4.5 The critical temperature versus modified exchange in $(\Delta_s - k_B T/J_3)$ phase planes for the films with different $L = 4,5,6,7$ layers. Two set of curves correspond to the selected amplitude agents $h_0/J_3 = 1.0, 2.5$. The number accompanying each panels denote the value of frequency $\omega = 0.1, 0.25, 0.5, 1.0, 2.0, 4.0$. Differences in the layer hierarchy on both sides of the crossover point is shown by the arrows in opposite directions. The exemplary inset of the crossover point is stated as visuality purposes.

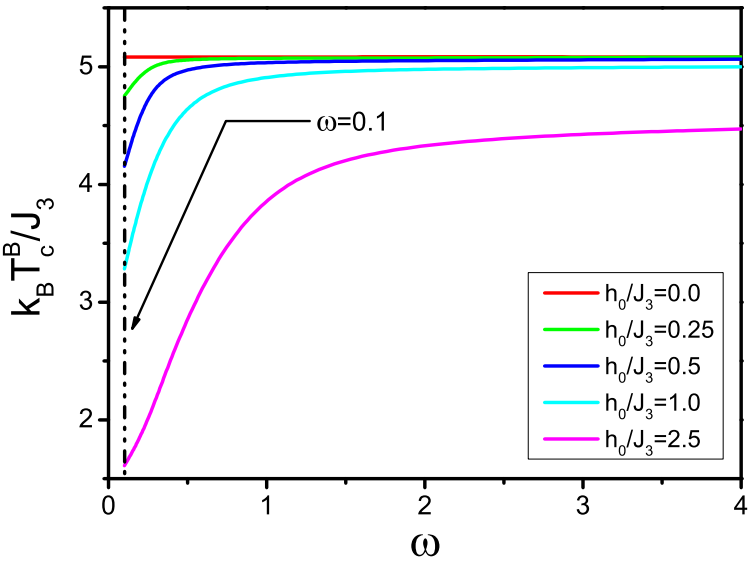

Figure 4.6 The frequency dispersion of the critical temperature coordinate of special point for different values of amplitudes $h_0/J_3 = 0.0, 0.25, 0.5, 1.0, 2.5$. The dashed line at $\omega = 0.1$ serves as a boundary for quasistatic limit. The curves are not depend on thickness of the film.

The frequency dispersions of the critical temperature coordinates of special point for various external oscillatory field amplitudes as $h_0/J_3 = 0.0, 0.25, 0.5, 1.0, 2.5$ can be shown in Fig. 4.6. In accordance with our anticipations, the dispersion curves evolve out of the characteristic line which accounts for the pure bulk system in quasitatic limit as rising h_0/J_3. The behavior of the dispersions qualitatively supports the last parts of the descriptions in the previous paragraph that is to say all dispersion curves saturates to the value of bulk critical temperature in $\omega \to \infty$ limit. Contrary to this, they go to a finite non-zero value in $\omega \to 0$ limit. Major attention was paid to catch the overall behavior of a dynamical thin film in our calculations, hence the lowest value of the frequency $\omega = 0.1$ was regarded as quasistatic limit in the treatment. This value is sufficient for estimation for the existence of the HL residuality mentioned above even now. The results given in this section are essentially based on the paper of us (Aktaş et al., 2014).

CHAPTER FIVE
RESULTS PART-2: DYNAMIC HYSTERETIC FEATURES

Hysteretic behavior is, however, a complicated process of a dynamic and nonlinear nature that eludes serious treatment, both experimentally and theoretically since the area enclosed by the hysteresis loop (HL) is directly proportional to the energy loss in a magnetization-demagnetization cycle. Low coercivity, which means low hysteresis loss per cycle of operation, is desired in core materials (or it is only used for a temporal magnetic recording). Contrary to this, high coercivity is used in applications where the magnetic recording media is frequently used or the long-lifetime recording is needed. This strategy is the main trend-setter in magnetic thin film design (Osaka et al., 2005). Controlling thickness of film to obtain the magnetic hysteresis at a right shape to suit desired technological purpose is the key issue in disguise (Suen & Erskine, 1997). Therefore, how the spontaneous spin formation mechanism involves in these reduced structures becomes the focus of frequent investigation issues. Due to the underlying complexity of reduced dimension, any systematic investigation regarding the hysteresis behavior and its influences on each layer are not exist. So, there are some important issues which remain in suspense; frequency dispersion of HLA with corresponding remanence and coercivity for different layer indices, classification of dispersion curves, topological evolution of the hysteretic response of each layer with varying the modified surface exchange, etc.

In this part, in order to understand and clarify the behavior of the system under consideration, the remanent magnetization (in other words residual magnetization which is the magnetization left behind in the system after the external magnetic field is removed) and coercive field (which means that the intensity of the external magnetic field needed to change the sign of the magnetization) has been calculated for a pure crystalline ferromagnetic thin film with $L = 7$ layers are presented in Figs. 5.1, 5.2 and 5.3. We see that the frequency dependency in each characteristic has a crossover at a critical value of modified exchange interaction Δ_s^*. There exists a hierarchical change of the HLA sequence for each layer in two different regimes of Δ_s as shown in Fig.

5.1. For a fixed h_0, the hysteresis loop of surface has the lowest area in $\Delta_s < \Delta_s^*$ regime till the symmetry loss. In other regime ($\Delta_s > \Delta_s^*$) the hysteresis loop of innermost layer has the lowest area. The layer indices are of no importance in frequency dependency at the critical value of modified exchange interaction. In other words, all the layers have the same hysteretic behavior at Δ_s^*. Physical mechanism can be briefly explained as follows: When proceeding from the surface to the center of the film, hysteresis loop becomes larger at lower ω but it slightly gets smaller at higher ω values for the fixed value of h_0 in $\Delta_s < \Delta_s^*$ regime. There are relatively more neighboring per magnetic-sites which causes locally larger magnetic interaction in inner layers. So, it becomes more difficult to follow the external field for any spin. Hysteresis is more likely to be asymmetric in this regime. Surface spins are embedded in an environment of lower symmetry than that of the inner atoms. The exchange constant between atoms in the surface region may differs from the bulk one. The lower Δ_s regime corresponds to surface type of magnetic ordering with this aspect. The opposite of the above scenarios can be considered also. From a different point of view, if the Δ_s increases (i.e. we are in $\Delta_s > \Delta_s^*$ regime now), hysteresis loop becomes smaller at low ω but slightly gets larger at high ω when proceeding from the surface to the center of the film. This is since for inner layers there are more neighboring but far fewer exchange constant per magnetic-sites which causes relatively smaller magnetic interaction than that of the surface one anymore. Eventually, the free surface can not breaks the translational symmetry since the hysteretic and/or magnetic properties of the free surfaces exactly overlap with the bulk one at the critical value of surface exchange Δ_s^*. We can say more generally that the deficiency of the interaction strength per surface spin can be compensated by increasing the modified exchange interaction strength. The coercivity and remanent magnetization presented in Figs. 5.2 and 5.3 are also consistent with the aforementioned arguments about the mechanism. They profiles across the film differ qualitatively in two regimes ($\Delta_s < \Delta_s^*$ and $\Delta_s > \Delta_s^*$).

A_k increases at low ω values first and then it reaches the maximum value in agreement with the well-known behavior in literature where frequency at the peak ω_M corresponds to the phase-lag. After ω_M, the hysteresis is in still purely symmetric region with reversed shape for a while. In $\Delta_s < \Delta_s^*$ regime, ω_M shifts to lower values with increasing layer index k (it means we are penetrating from the surface to the center) due to the locally stronger magnetic interaction. A_k is also increases (especially at low ω) with increasing layer index k for fixed ω in the same regime of Δ_s. The opposite of all these arguments can be also thought for $\Delta_s > \Delta_s^*$ regime. One can easily observe the intersection of layers via changing Δ_s parameter at ω_M. One can easily follow from Figs. 5.2 and 5.3 respectively, the coercivity $H_c^{(k)}$ is relatively large for larger field amplitude h_0. The effect of larger field amplitude h_0 on remanence $M_r^{(k)}$ can be seen also in asymmetric region. A_k increases with increasing h_0 and this increment is independent of the other system parameters. This is since the magnetic energy due to the energy supplied by the external field in a cycle automatically becomes higher for higher amplitude values. This higher energy provides more magnetic force which increases the ability of the spins to follow the external field sweep. Consequently, corresponding frequency for the maximal peak (ω_M) in symmetric region and value of Δ_s shifts to higher frequencies. It is clear that the phase-lag between magnetization time-series and external field signal is smaller for the higher amplitude.

The hysteresis loop collection of each layer for the selected system parameters together with three appropriate values of frequency are presented in Fig. 5.4. In the low frequency limit, the magnetization can be more saturated and this shows itself as dominant magnetization processes in the different regions of the hysteresis (i.e. reversible boundary displacements, irreversible boundary displacements and magnetization rotation). The figure shows that the hysteretic response of each layer clearly has the same characteristics at the critical value of the modified exchange Δ_s^* independently from the other parameters. Hierarchically changing the order of the hysteresis loop for various values of amplitudes and/or frequency also can be seen in Fig. 5.4 by following the group of three columns including the related regimes of Δ_s ($\Delta_s < \Delta_s^*$, $\Delta_s \equiv \Delta_s^*$ and $\Delta_s > \Delta_s^*$). One can observe the symmetry process on

this order changing (corresponds to the following ability of the spin to external field sweep) by comparing the representative amplitudes between each other. For Δ_s^* value and $h_0 = 2.5$ representative, the hysteresis loop has a saturated s-shape and tends to enhance its size with increasing ω at low frequency region e.g. $\omega < 0.3$. However, on further increasing ω, the loop gets its maximum area and later on reduces to an oval shape with its major axis parallel to the field axis. This is the result of phase-lag between the magnetization time-series and the field signal. At very low ω, the field period is large and the magnetic spins have sufficient time to follow the field signal so the phase-lag between the magnetization time-series and field signal is very small. The system is strong enough to follow the external perturbation at those limitations, hence the hysteresis loop looks like a slim s-shape. However, on increasing ω, the field sweeps faster. But, the relaxation time of the system is fixed, so spins still have less time to follow the field. Phase-lag gets larger and so does the HLA. While the frequency value is approaching to correspondence phase-lag, the hysteresis gets its maximum size which corresponds to the frequency ω_M. After that, if ω still increases in small doses, the system can not follow the field and the spins do not align in the same direction with external oscillatory field in each moment of a full cycle. Finally, the hysteresis dramatically loses its symmetry at a certain ω_C value. For $h_0 = 1.0$, a rare hysteresis shape and symmetry loss with increasing frequency can be seen by following the aforementioned topological evolution at the fixed $\Delta_s > \Delta_s^*$. For instance, as seen at $\omega = 0.07$, an exotic left-handed s-shape beyond the oval form temporally takes place between corresponding maximal area frequency ω_M and the frequency value of symmetry loss ω_C where $\omega_C > \omega_M$. The general trend mainly can be also explained as follow: For low frequencies, the hysteresis loop is in the form of saturated s-shape and tends to enhance its size with increasing ω at low frequency region. At ω_M value, the loop gets its maximum area. With a further increase in frequency, hysteresis enters into the process of smooth directional-veering and it changes its shape to left-handed s-shape until the symmetry loss. Finally, the symmetry loss occurs at a characteristic frequency value ω_C, so the hysteresis has asymmetric shape anymore.

The process stated between at the beginning of directional-veering and symmetry loss (in between ω_M and ω_C) deserves a scrutiny in terms of magnetic domain nucleation. As seen in Figs. 5.1, 5.2 and 5.3, symmetry loss shows itself as a gibbous-like eminentia in ω_C. This phenomenon is also zoomed in Figs. 5.1 and 5.2 for better visibility. Particularly, as seen in Fig. 5.3, both positive and negative remanence appears at low frequencies, but only positive values survive at high frequencies. This is also another indication of symmetry loss. The related eminentia shows itself more clearly on right arm of the mutual coercivity and it is more and more distinct in surfaces for low amplitudes especially in $\Delta_s > \Delta_s^*$ regime. We note that the encountered characteristics on this problem are the member of Type II.b family of frequency dispersion presented by Aktaş et al. (Aktaş et al., 2012).

As we mentioned above, low amplitude relatively provides smaller magnetic energy to the system and this weak energy could not provide enough magnetic force in causing the spins to follow the field. This means that the surfaces fall all over itself to adopt to the asymmetric phase in the $\Delta_s > \Delta_s^*$ regime. So, the surfaces have extremely left-handed saturated s-shape hysteretic response within that period. It is also an special interest to consider the topological evolution of the hysteresis with varying ω to investigate how it relates with spin formation (magnetic domains) growth and/or nucleation mechanism. Two branches of the hysteresis are almost lie on two perpendicular directions at ω_M. HLA has its maximum area which is related to these two axis and their orientation. Therefore, the magnetic moments remain a constant value in the half-time period of external field at this frequency ω_M. At the fixed values of $\omega < \omega_M$ and $\omega > \omega_M$ respectively, corresponding hysteresis curves are topologically contra-oriented and completely different growth mechanisms are onset. The importance of this left-handed shape on the domain mechanism is that the domains currently continue to nucleate in a direction with a delay, while the magnetic field is increasing in the opposite direction in a half period of full cycle. This phenomenon should be considered especially on the fabrication process of thin films for magnetic recording purposes. Magnetization time-series versus the external magnetic field, increasing the field frequency at first, obstructs the saturation of the

ordinary magnetization due to the decreasing energy coming from the oscillating magnetic field in the half-time period which facilitates the late stage domain growth by tending to align the moments in its direction (i.e. the magnetization is no longer able to follow the oscillatory field). This enables a frequency increasing route to continuous DPT due to the incomplete reversal of magnetic moments.

The aforementioned directional-veering mechanism begins to lose its significance in the $\Delta_s < \Delta_s^*$ regime. When the Δ_s is lowered more and more, the dipole-dipole interaction-induced energy contribution becomes smaller. The strength of the energy contribution which comes from the dipole-dipole interaction corresponds to remain in dynamically symmetric phase of the system's own volition. Hence, the surfaces can stay in the symmetric phase in the smaller frequency until the frequency of the external field becomes greater than the intrinsic relaxation time of the system. The results given in this section are essentially based on the paper of us (Aktaş et al., 2015).

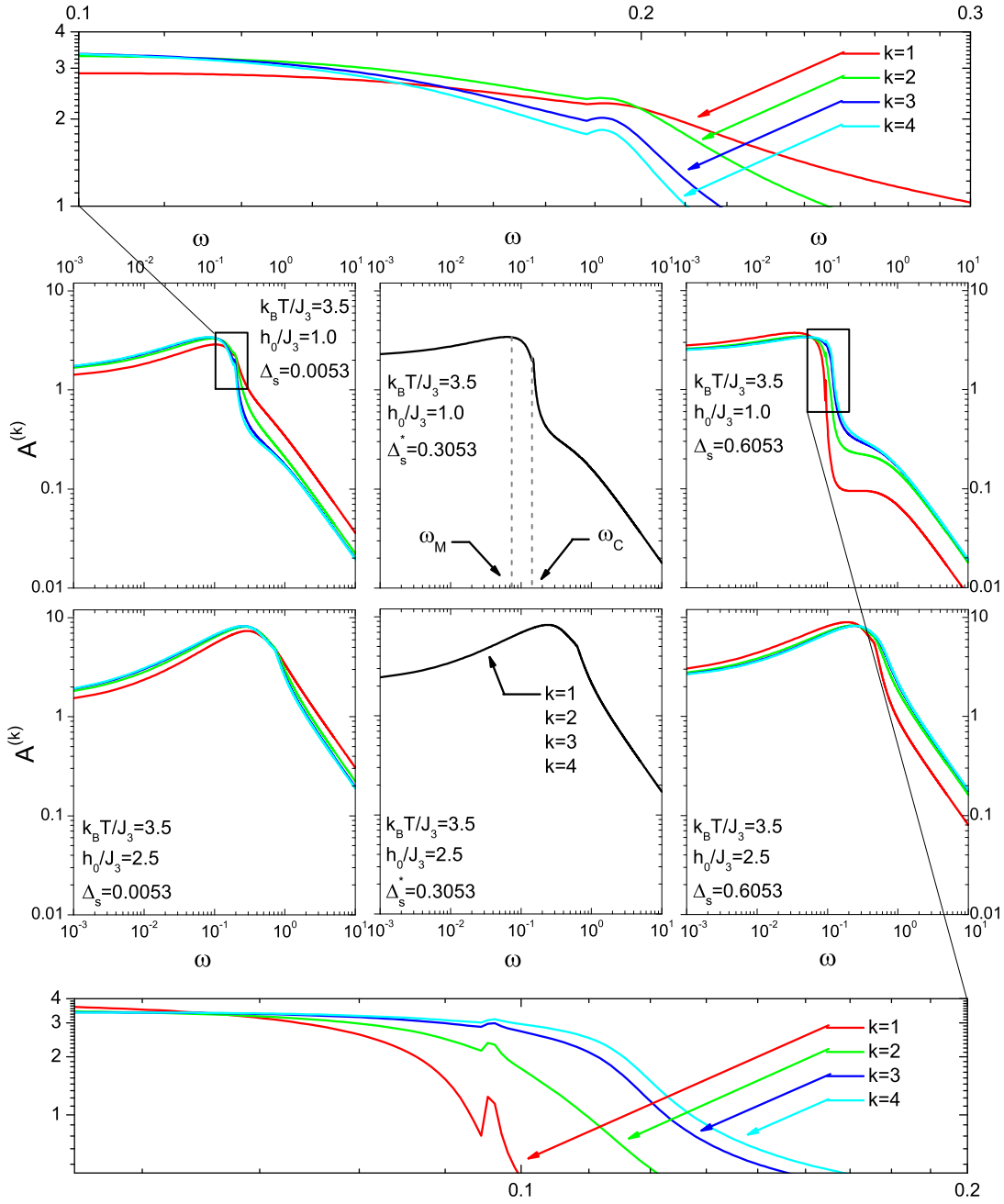

Figure 5.1 The frequency dispersion of HLA for each layer of $L = 7$ at a fixed temperature $k_BT/J_3 = 3.5$. The curves were plotted for the selected amplitude representatives as $h_0 = 1.0$ and 2.5 in each group of triple-column. The sequence of dispersions is reversed in two different regimes of modified exchange interaction.

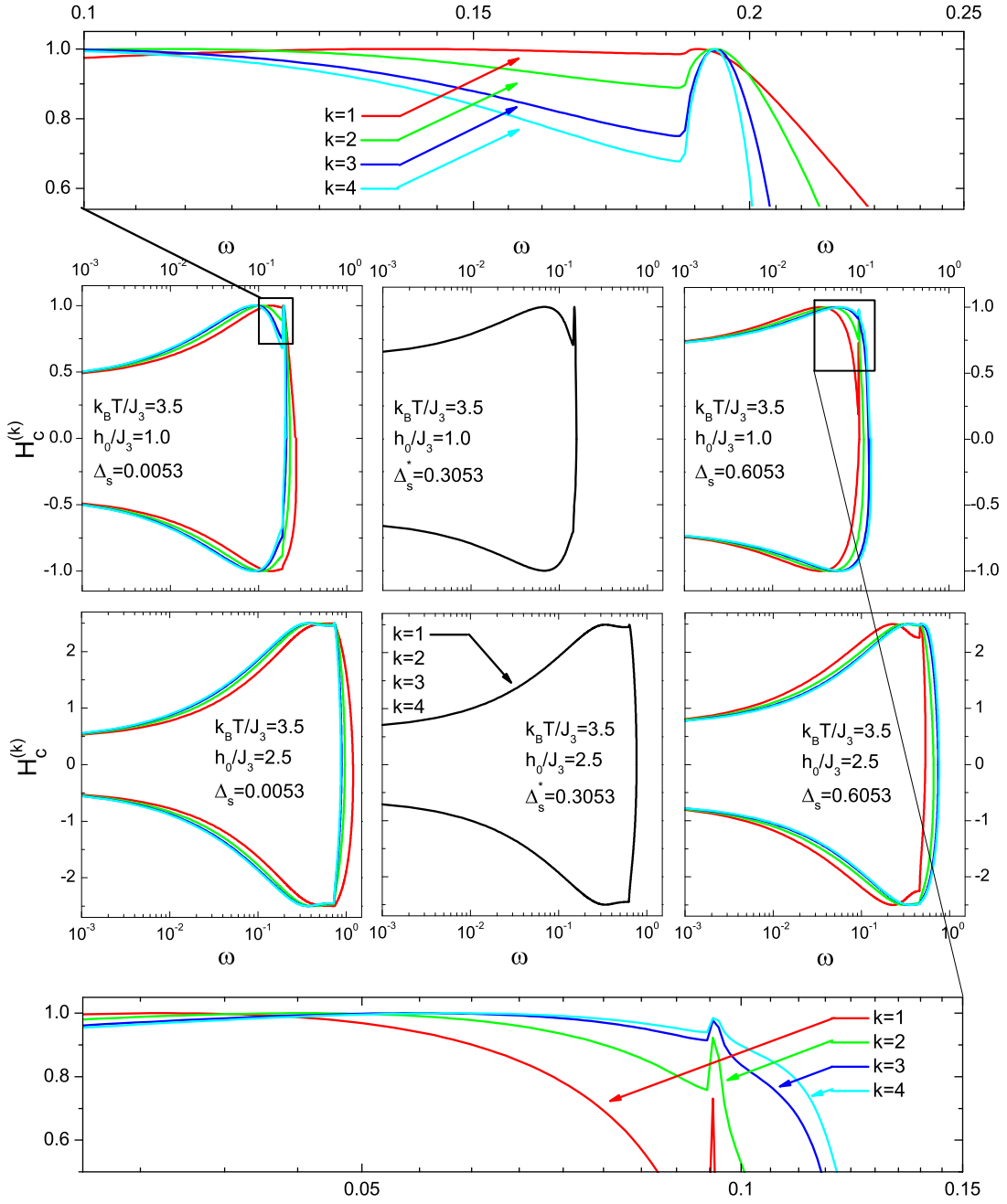

Figure 5.2 The frequency dispersion of coercive field for the same selected system parameters of the film depicted in Fig. 5.1. The sequence of dispersions is reversed in two different regimes of modified exchange interaction.

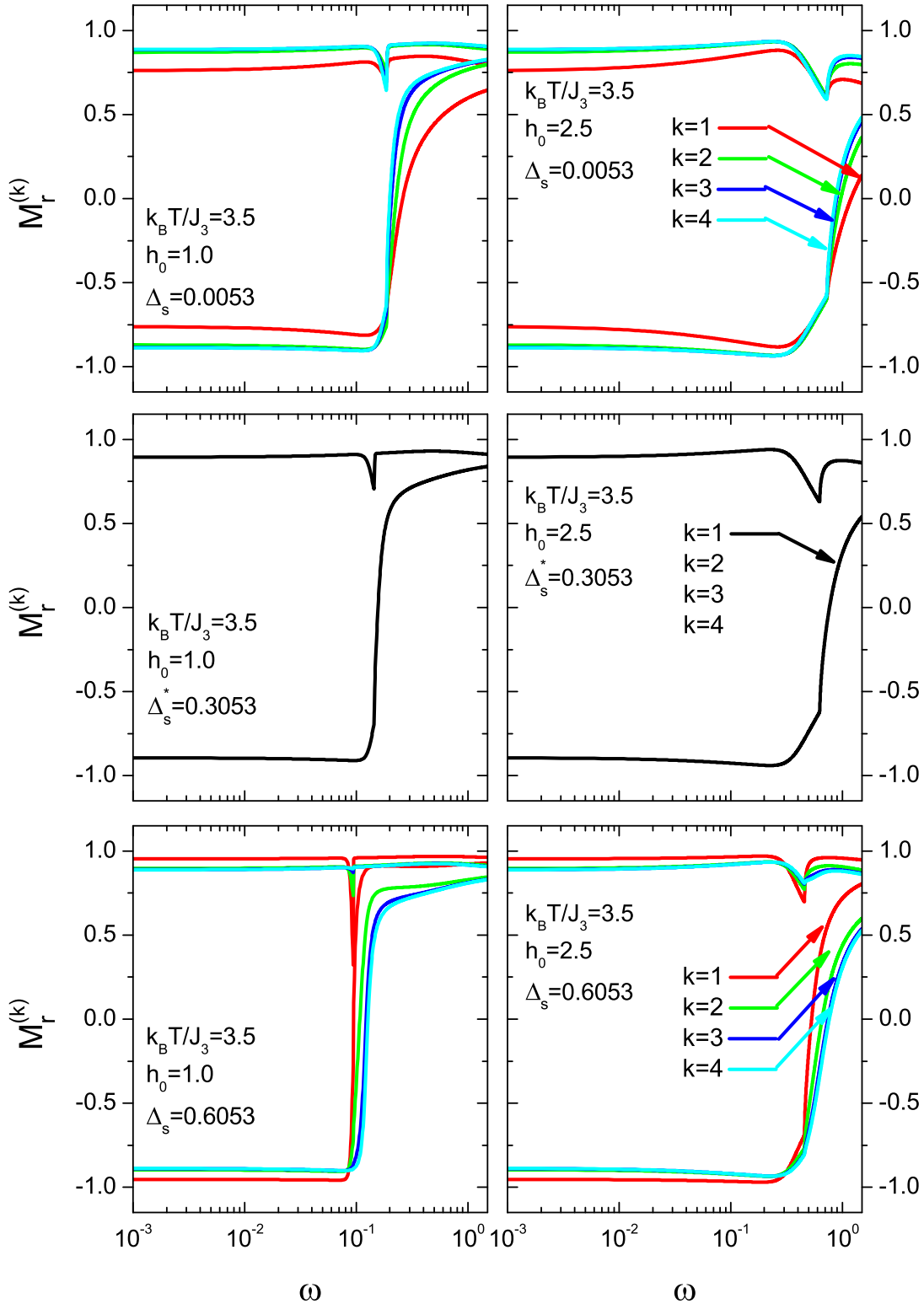

Figure 5.3 The frequency dispersion of remanent magnetization for the same selected system parameters of the film depicted in Fig. 5.1. The sequence of dispersions is reversed in two different regimes of modified exchange interaction.

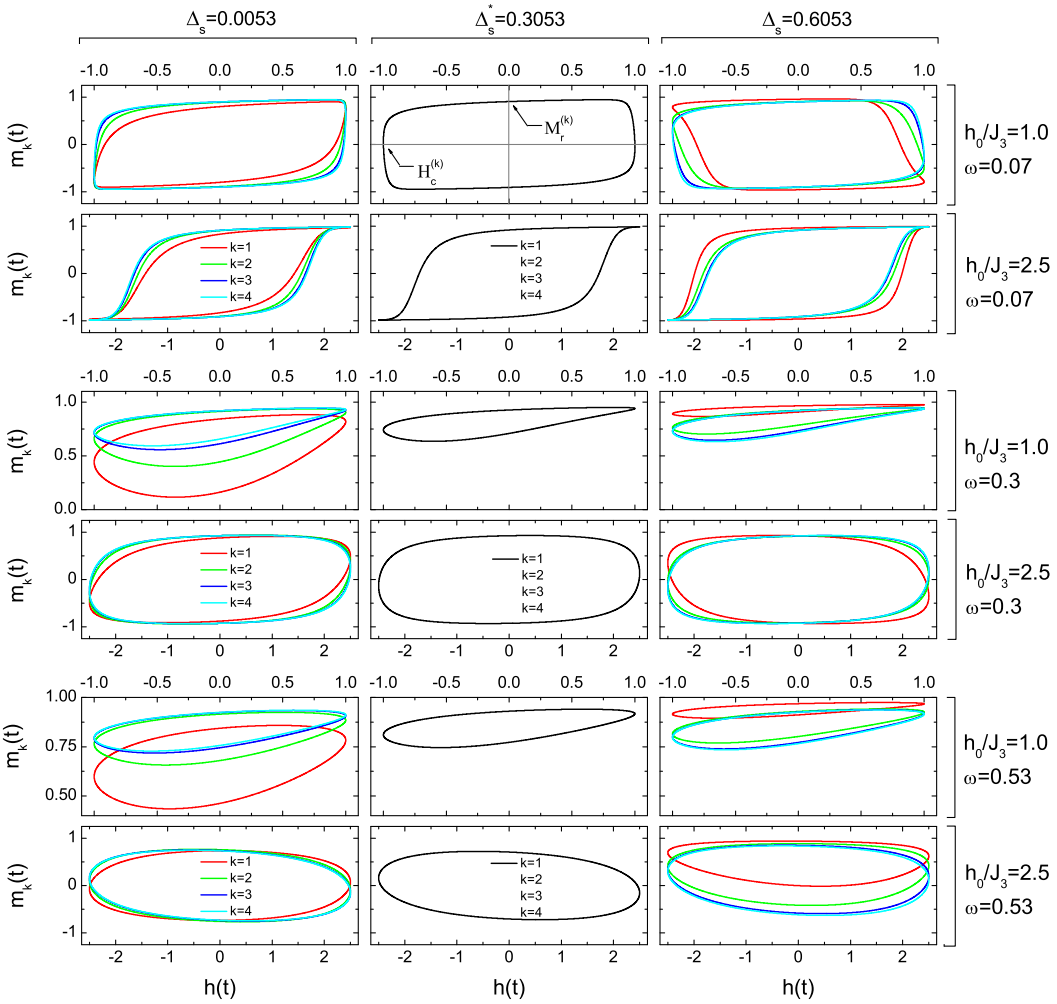

Figure 5.4 Well-selected hysteresis collection of each layer for the film with thickness $L = 7$. Modified exchange interaction Δ_s ranges from 0.0053 (first column) to 0.3053 (second column) and 0.6053 (third column) with varying frequency as $\omega = 0.07$, 0.3 and 0.53 for related amplitude representatives at $k_BT/J_3 = 3.5$. The reader can recognize the hierarchical evolution. Here, we note that the surface loop ($k = 1$) is more saturated in any case for $\Delta_s < \Delta_s^*$ value and the sequence of hysteresis is reversed in two different regimes of modified exchange interaction.

CHAPTER SIX
CONCLUSION

In this thesis, we first investigate the surface enhancement phenomenon and dynamic nature of the critical phenomena which was observed for dynamical Ising-typed thin films with various thicknesses defined with inner coordination number $z = 4$ and driven by an external oscillatory magnetic field by means of EFT based on a standard decoupling approximation. The time evolution of the system was presented by utilizing a Glauber type stochastic process.

As it is well known, coercivity for a fixed temperature is directly related with varying frequency and amplitude of the external field. While an information being saved magneto-optically, one needs to consider the optimization of coercivity which is directly proportional to the energy loss in a magnetization-demagnetization cycle, order-disorder transition point, the relation between frequency/amplitude and film thickness, etc. Although, the aforementioned properties is the subject of our followup examination on this system, in this study we had to elucidate the evolution of the static properties of the magnetic thin film with respect to the external oscillatory perturbation parameters, e.g., fundamentally temperature dependency of DOP (ordinary magnetization for a dynamical system), the average magnetization of each layer, related global phase diagrams and ultimately frequency dispersion can be seen in the figures of our work respectively. Mainly for this purpose, our starting point for the systematic review was to examine the DOP, average magnetization of layers with respect to temperature and layer index for the selected field amplitude and frequency values at finite temperature below the Curie point of the static case for a pure Ising-typed bulk. The effect of the frequency and amplitude on the standard arguments were propounded. For this purpose, the most appropriate values and/or intervals of parameters were chosen for the treatment. We supported the relevant investigations with phase diagrams globally in addition to the average magnetization.

In order to examine the effect of the dynamical parameters of external field on the phase diagrams, the phase diagrams for selected three distinct modified

exchange representatives with three values of frequency were presented in ($h_0/J_3 - k_BT/J_3$) planes. In the immediate aftermath, the frequency induced evolution of the corresponding agents along the routes at $h_0/J_3 = 1.0, 2.5$ respectively in the previous phase diagrams were investigated at finite temperature in ($\Delta_s - k_BT/J_3$). According to our findings, a weak decreasing of the amplitude causes decreasing in Δ_s coordinate of the crossover point, while a small increment of the frequency causes an increment critical temperature component of the crossover. For a better view, we have depicted frequency dispersion of the k_BT_c/J_3 coordinate of the special point for aforementioned amplitude agents.

The second part focuses on the frequency dispersion of HLA, coercivity, and the remanence of each layer for a film with fixed thickness.

In order to find out the physical relation between domain growth and/or nucleation mechanism and symmetry loss, the topological evolution of the hysteresis with varying frequency is considered. Hence, some unpretentious improvements are developed in accordance with the explanations given before in literature (Jiang et al., 1995; He & Wang, 1993; Suen et al., 1999; Laosiritaworn, 2009).

The existence of a special transition point presented in Ref (Aktaş et al., 2014) has been already confirmed by Tauscher and Pleimling via both Glauber and Metropolis dynamics (Tauscher & Pleimling, 2014). Moreover, one can find to be of another interest is the existence of a critical value of the surface exchange parameter at which all the layers seem to oscillate in phase. Based on the Monte Carlo results (Tauscher & Pleimling, 2014), we can say that the existence a crossover in all hysteretic characteristics are not from the limitation of the method. This would hopefully provide some theoretical insight into the role of the surface layer and possibly some guidance to experimental studies on such systems.

Especially the short-time reversed shape of hysteresis in the frequency-induced evolution which can only be recognized with such detailed examination as obtained from this work is another issue worth considering.

EFT takes the standard MFA predictions one step forward by taking into account the single spin correlations which means that the thermal fluctuations are partially considered. Although all of the observations reported in this work shows that EFT can be applied to such nonequilibrium realistic systems, the true nature of the physical facts underlying the observations displayed in the system (especially the origin of the different contrary effects of two variables of the external filed related between the competing time scales) may be further understood with an improved version of the present EFT formalism which can be achieved by attempting to consider the multi spin correlations which originate when expanding the spin identities or a MC simulation as stochastic process. We believe that this attempt could provide a treatment beyond the present approximation. The main result that the reader would find to be of interest is the existence of a critical value of the surface exchange parameter at which all the layers seem to oscillate in phase, i.e., this investigation in the interest of saving time for experimental data getting by trial and error. For all these reasons, it also could be helpful as a guide for experimentally investigation of the crossover phenomena in this dynamical problem.

In conclusion, we hope that the collectively presented results of our study would shed light on the further investigations of the dynamic nature of the critical phenomena in pure crystalline systems (e.g. thin films and semi-infinite systems) and would be beneficial from both theoretical and experimental points of view.

REFERENCES

Aguilera-Granja, F., & Morán-López, J. L. (1985). Mean-field theory of magnetic transitions in semi-infinite Ising models. *Physical Review B*, *31*(11), 7146.

Akıncı, Ü. (2013). Effects of the randomly distributed magnetic field on the phase diagrams of the transverse Ising thin film. *Journal of Magnetism and Magnetic Materials*, *329*, 178.

Aktaş, B. O., Akıncı, Ü., & Polat, H. (2012). Hysteretic response characteristics and dynamic phase transition via site dilution in the kinetic Ising model. *Physica B: Condensed Matter*, *407*(24), 4721.

Aktaş, B. O., Akıncı, Ü., & Polat, H. (2014). Critical phenomena in dynamical Ising-typed thin films by effective-field theory. *Thin Solid Films*, *562*, 680.

Aktaş, B. O., Akıncı, Ü., & Polat, H. (2015). Dynamic hysteretic features of ising-type thin films. *Physical Review E*, *407*(9), 4721.

Balcerzak, T. (1991). Cluster identities in localized spin systems. *Journal of Magnetism and Magnetic Materials*, *97*, 152.

Baxter, R. J. (1982). *Exactly solved models in statistical mechanics.* (1st ed.). London and San Diego: Academic Press.

Binder, K. (1974). Monte Carlo study of thin magnetic Ising films. *Thin Solid Films*, *20*, 367.

Binder, K., & Hohenberg, P. C. (1974). Surface effects on magnetic phase transitions. *Physical Review B*, *9*(5), 2194.

Colombo, E., Donzelli, O., Fratucello, G. B., & Ronconi, F. (1992). Static magnetization direction in fcc (111) Fe/Ni multilayers. *Journal of Magnetism and Magnetic Materials*, *104*, 1857.

Cossio, P., Mazo-Zuluaga, J., & Restrepo, J. (2006). Critical behavior of ferromagnetic Ising thin films. *Physica B*, *384*, 227.

Detzel, T., Vonbank, M., Donath, M., Memmel, N., & Dose, V. (1996). Temperature-dependent magnetization of fcc Fe/Cu(001) studied by spin-polarized appearance potential spectroscopy. *Journal of Magnetism and Magnetic Materials*, *152*, 287.

Dürr, W., Taborelli, M., Paul, O., Germar, R., Gudat, W., Pescia, D., & Landolt, M. (1989). Magnetic Phase Transition in Two-Dimensional Ultrathin Fe Films on Au(100). *Physical Review Letters*, *62*(2), 206.

Edelstein, A. S., Kim, C., Qadri, S. B., Kim, K. H., Browning, V., Yu, H. Y., Maruyama, B., & Everett, R. K. (1990). Magnetic coupling in high moment f.c.c. Fe/Ni multilayers. *Solid State Communication*, *76*, 1379.

Etchegoin, P., & Nöllmann, M. J. (2003). A model for protein-DNA interaction dynamics. *Journal of Theoretical Biology*, *220*, 233.

Farle, M., & Baberschke, K. (1987). Ferromagnetic order and the critical exponent γ for a Gd monolayer: An electron-spin-resonance study. *Physical Review Letters*, *58*(5), 511.

Farle, M., Baberschke, K., Stetter, U., Aspelmeier, A., & Gerhardter, F. (1993). Thickness-dependent Curie temperature of Gd(0001)/W(110) and its dependence on the growth conditions. *Physical Review B*, *47*(17), 11571.

Glauber, R. J. (1963). Time-dependent statistics of the ising model. *Journal of Mathematical Physics*, *4*, 294.

He, Y. L., & Wang, G. C. (1993). Observation of dynamic scaling of magnetic hysteresis in ultrathin ferromagnetic Fe/Au(001) films. *Physical Review Letters*, *70*, 2336.

Honmura, R., & Kaneyoshi, T. (1979). Contribution to the new type of effective-field theory of the Ising model. *Journal of Physics C: Solid State Physics*, *12*, 3979.

Ising, E. (1925). Beitrag zur theorie des ferromagnetismus. *Zeitschrift fÃ¼r Physik*, *31*, 253.

Jiang, Q., Yang, H. N., & Wang, G. C. (1995). Scaling and dynamics of low-frequency hysteresis loops in ultrathin Co films on a Cu(001) surface. *Physical Review B*, *52*, 14911.

Jonker, B. T., Walker, K. H., Kisker, E., Prinz, G. A., & Carbone, C. (1986). Spin-polarized photoemission study of epitaxial Fe(001) films on Ag(001). *Physical Review Letters*, *57*(1), 142.

Kaneyoshi, T. (1980). Comments on molecular-field theory with correlations. *Physics Letters A*, *76*(1), 67.

Kaneyoshi, T. (1991). Surface magnetism; magnetization and anisotropy at a surface. *Journal of Physics: Condensed Matter*, *3*, 4497.

Kaneyoshi, T., Honmura, R., Tamura, I., & Sarmento, E. F. (1984). Amorphization of a crystalline diluted Ising ferromagnet. *Physical Review B*, *29*, 5121.

Kaneyoshi, T., Tamura, I., & Sarmento, E. F. (1983). Surface magnetic properties of the Ising model with a diluted free surface. *Physical Review B*, *28*(11), 6491.

Kaufman, B., & Onsager, L. (1949). Crystal statistics. iii. short-range order in a binary Ising lattice. *Physical Review*, *76*, 1244.

Krishnan, R., Gupta, H. O., Lassri, H., Sella, C., & Kaabouchi, M. (1991). Structural and magnetic properties of Fe/Ni and Fe/Co multilayers. *Journal of Applied Physics*, *70*, 6421.

Landau, D. P., & Binder, K. (1990). Monte Carlo study of surface phase transitions in the three-dimensional Ising model. *Physical Review B*, *41*(7), 4633.

Laosiritaworn, Y. (2009). Monte Carlo simulation on thickness dependence of hysteresis properties in Ising thin-films. *Thin Solid Films*, *517*, 5189.

Laosiritaworn, Y., Poulter, J., & Staunton, J. B. (2004). Magnetic properties of Ising thin films with cubic lattices. *Physical Review B*, *70*, 104413–1–9.

Li, Y., & Baberschke, K. (1992). Dimensional crossover in ultrathin Ni(111) films on W(110). *Physical Review Letters*, *68*(8), 1208.

Li, Y., Polaczyk, C., Klose, F., Kapoor, J., Maletta, H., Mezei, F., & Riegel, D. (1996). Magnetic and structural properties of thin Fe films grown on Ni/Si. *Physical Review B*, *53*(9), 5541.

Mahan, G. D., & Francisco, H. C. (1977). Ising model with magnetic field and the lattice gas. *Physical Review B*, *16*, 1168.

Onsager, L. (1944). Crystal statistics. i. A two-dimensional model with an order-disorder transition. *Physical Review*, *65*, 117.

Osaka, T., Asahi, T., Kawaii, J., & Yokoshima, T. (2005). Development of high-performance magnetic thin film for high-density magnetic recording. *Electrochimica Acta*, *50*, 4576.

Pappas, D. P., Kämper, K. P., & Hopster, H. (1990). Reversible transition between perpendicular and in-plane magnetization in ultrathin films. *Physical Review Letters*, *64*(26), 3179.

Park, H., & Pleimling, M. (2012). Surface criticality at a dynamic phase transition. *Physical Review Letters*, *109*, 175703–1–5.

Pescia, D., Stampanoni, M., Bona, G. L., Vaterlaus, A., Willis, R. F., & Meier, F. (1987a). Magnetism of epitaxial fcc iron films on Cu(001) investigated by spin-polarized photoelectron emission. *Physical Review Letters*, *58*(20), 2126.

Pescia, D., Zampieri, G., Stampanoni, M., Bona, G. L., Willis, R. F., & Meier, F. (1987b). Ferromagnetism of thin epitaxial fcc cobalt films on Cu(001) observed by spin-polarized photoemission. *Physical Review Letters*, *58*(9), 933.

Pierce, D. T. (1987). Experimental studies of surface magnetism with polarized electrons. *Surface Science*, *189*, 710.

Poulopoulos, P., & Baberschke, K. (1999). Magnetism in thin films. *Journal of Physics: Condensed Matter*, *11*, 9495.

Przybylski, M., & Gradmann, U. (1987). Ferromagnetic order in a Fe(110) monolayer on W(110) by Mössbauer spectroscopy. *Physical Review Letters*, *59*(10), 1152.

Rau, C., & Eichner, S. (1981). Electron-spin polarization at single-crystalline Cr and Ni surfaces determined with electron-capture spectroscopy. *Physical Review Letters*, *47*(13), 939.

Rau, C., Jin, C., & Robert, M. (1988). Ferromagnetic order at Tb surfaces above the bulk Curie temperature. *Journal of Applied Physics*, *63*, 3667.

Reichl, L. E. (1997). *A modern course in statistical physics*. (2nd ed.). A Wiley-Interscience Publication.

Saber, M., Ainane, A., Dujardin, F., & Stebe, B. (1999). Magnetic properties of a transverse spin-1/2 Ising film. *Physical Review B*, *59*(10), 6908.

Schneider, C. M., Bressler, P., Schuster, P., Kirschner, J., de Miguel, J. J., & Miranda, R. (1990). Curie temperature of ultrathin films of fcc-cobalt epitaxially grown on atomically flat Cu(100) surfaces. *Physical Review Letters*, *64*(9), 1059.

Stampanoni, M. (1989). Magnetic properties of thin epitaxial films investigated by spin-polarized photoemission. *Applied Physics A: Materials Science and Processing*, *49*, 449.

Stampanoni, M., Vaterlaus, A., Aeschlimann, M., & Meier, F. (1987). Magnetism of Epitaxial bcc Iron on Ag(001) Observed by Spin-Polarized Photoemission. *Physical Review Letters*, *59*(21), 2483.

Suen, J. S., & Erskine, J. L. (1997). Magnetic hysteresis dynamics: Thin p(1×1) Fe films on flat and stepped W(110). *Physical Review Letters*, *78*, 3567.

Suen, J. S., Lee, M. H., Teeter, G., & Erskine, J. L. (1999). Magnetic hysteresis dynamics of thin Co films on Cu(001). *Physical Review B*, *59*, 4249.

Tauscher, K., & Pleimling, M. (2014). Surface phase diagram of the three-dimensional kinetic Ising model in an oscillating magnetic field. *Physical Review E*, *89*, 022121.

Tomé, T., & de Oliveira, M. J. (1990). Dynamic phase transition in the kinetic ising model under a time-dependent oscillating field. *Physical Review A*, *41*, 4251.

Tucker, J. W. (1991). Effective field theory of dilute Ising systems. *Journal of Magnetism and Magnetic Materials*, *102*, 144.

Upton, P., & Yeomans, J. (1989). Model for binary alloys: An Ising model with isotropic competing interactions. *Physical Review B*, *40*, 479.

Vatansever, E. (2011). *Spin sistemlerinin denge yakınlarındakı kinetik davranışlarının íncelenmesi*. MSc Thesis, Dokuz Eylül University, Graduate School of Natural and Applied Sciences, Ízmir.

Wang, Y. G., Zhong, W. L., & Zhang, P. L. (1997). Ferroelectric films described by transverse Ising model with long-range interactions. *Solid State Communication*, *101*, 807.

Weller, D., Alvarado, S. F., Gudat, W., Schröder, K., & Campagna, M. (1985). Observation of surface-enhanced magnetic order and magnetic surface reconstruction on Gd(0001). *Physical Review Letters*, *54*(14), 1555.

Yao, D.-L., Wu, Y.-Z., & Li, Z.-Y. (2002). Pyroelectric coefficient and dielectric susceptibility of a ferroelectric bilayer with an antiferroelectric interfacial coupling. *Physica Status Solidi (b)*, *231*, 561.

Yeomans, J. M. (1993). *Statistical mechanics of phase transition*. (2nd ed.). Oxford: Oxford University Press.

Yüksel, Y. (2013). *Improved effective field theory analysis of critical phenomena in Ising model with quenced disorder effects*. PhD Thesis, Dokuz Eylül University, Graduate School of Natural and Applied Sciences, Ízmir.

Zaim, A., Amraoui, Y. E., Kerouad, M., & Arhchoui, H. (2008). Monte Carlo study of the spin-1 Blume-Capel Ising film. *Journal of Magnetism and Magnetic Materials*, *320*, 1030.

Zernike, F. (1940). The propagation of order in Co-operative phenomena: Part i. the AB case. *Physica*, *7*(7), 565.